CrossMark

Warming and Elevated CO_2 Have Opposing Influences on Transpiration. Which is more Important?

Miko U. F. Kirschbaum[1] · Andrew M. S. McMillan[1]

Abstract

Plant transpiration is a key component of the terrestrial water cycle, and it is important to understand whether rates are likely to increase or decrease in the future. Plant transpiration rates are affected by biophysical factors, such as air temperature, vapour pressure deficits and net radiation, and by plant factors, such as canopy leaf area and stomatal conductance. Under future climate change, global temperature increases, and associated increases in vapour pressure deficits, will act to increase canopy transpiration rates. Increasing atmospheric CO_2 concentrations, however, is likely to lead to some reduction in stomatal conductance, which will reduce canopy transpiration rates. The objective of the present paper was to quantitatively compare the importance of these opposing driving forces. First, we reviewed the existing literature and list a large range of observations of the extent of decreasing stomatal conductance with increasing CO_2 concentrations. We considered observations ranging from short-term laboratory-based experiments with plants grown under different CO_2 concentrations to studies of plants exposed to the naturally increasing atmospheric CO_2 concentrations. Using these empirical observations of plant responses, and a set of well-tested biophysical relationships, we then estimated the net effect of the opposing influences of warming and CO_2 concentration on transpiration rates. As specific cases studies, we explored expected changes in greater detail for six specific representative locations, covering the range from tropical to boreal forests. For most locations investigated, we calculated reductions in daily transpiration rates over the twenty-first century that became stronger under higher atmospheric CO_2 concentrations. It showed that the effect of CO_2-induced reduction of stomatal conductance would have a stronger transpiration-depressing effect than the stimulatory effect of future warming. For currently cold regions, global warming would, however, lengthen the growing seasons so that annual sums of transpiration could increase in those regions despite reductions in daily transpiration rates over the summer months.

Keywords CO_2 · Evaporation · Evapotranspiration · Global change · Penman-Monteith · Stomata · Temperature

Introduction

Climate change is now well recognised as an important environmental change that will shape our future. The most certain change is an increase in the atmospheric CO_2 concentration ($[CO_2]$). While most attention has been focused on the radiative consequences of increasing $[CO_2]$ in the atmosphere [1],

$[CO_2]$ also has direct effects on plant growth and function [2–4]. This can be seen in short-term photosynthetic responses [5], growth responses in short-term experiments [6••], growth responses in the field under artificially increased $[CO_2]$ [7, 8] and in global patterns, such as reductions in river runoff [9].

CO_2-response studies most commonly provide plants with adequate access to soil water. Under water-limited conditions, however, relative plant growth responses to elevated $[CO_2]$ can potentially be even greater because increases in photosynthesis and decreases in stomatal conductance can together enhance water use efficiency to a numerically greater extent than the photosynthetic enhancement alone. This has led to the theoretical consideration that water plants grown with a limited water supply should respond more strongly to elevated $[CO_2]$ than plants grown with adequate soil moisture [10].

✉ Miko U. F. Kirschbaum
KirschbaumM@LandcareResearch.co.nz

[1] Landcare Research, Private Bag 11052, Palmerston North 4442, New Zealand

The other likely climatic change is an increase in global temperature [1], with the extent of temperature increases depending on the magnitude of increases in greenhouse gas concentrations. They can be described through different representative concentration pathways (RCPs), with future scenarios typically described as one of four scenarios, RCP 2.6, RCP 4.5, RCP 6.0 or RCP 8.5 [11], with the respective numbers describing the increase in radiative forcing by the end of the twenty-first century. Anticipated temperature increases are expected to vary across the globe, with smaller increases expected for the tropics and larger increases at high latitudes [1].

Increasing temperature is expected to increase evaporative demand because warmer air can hold more moisture. Provided the relative humidity remains the same, as has been observed to date [12], vapour pressure deficits (VPDs) will increase with warming by about 5–6%°C^{-1} [13], and that will drive increases in evapotranspiration rates [13–15]. While increasing temperature and VPD are the underlying driving forces for increases in evapotranspiration rates, the ultimate magnitude of changes in transpiration rates will be determined by the interplay between the increases in temperature and VPD and the canopy properties that control their heat and water vapour exchanges [13, 15].

In assessing future rates of water loss, it is important to distinguish between evaporation and transpiration, which together can be referred to as evapotranspiration. Evaporation refers to the evaporation of surface water, which can be from open water bodies, soil surfaces or from plant canopies if they are wet after rainfall events. Evaporation rates do not directly depend on plant processes. Plants neither restrict evaporative water loss through partial stomatal closure nor enhance it through plant roots that bring water to the surface from where it could evaporate. The shading of the soil surface by plant canopies and the extent of water held on wet plant foliage are, however, important indirect processes that influence evaporation rates.

Transpiration (E_{Tr}), on the other hand, refers to the movement of water through living plants. Transpiration rates are controlled by the combined effects of biophysical drivers and stomatal conductance. Partial stomatal closure can greatly curtail transpiration rates compared with the evaporation from free water surfaces subject to the same biophysical drivers [16•, 17•]. However, plants can also facilitate water loss by accessing water deep within the soil profile so that transpiration can be sustained even when there is no available surface water.

Future evaporation rates are likely to increase, driven principally by increasing temperature and VPD that increase evaporative demand. Transpiration rates, however, will be curtailed by partial stomatal closure in response to increasing [CO$_2$] [13, 18]. Climate change thus has two opposing effects on transpiration rates: increased temperature enhances the biophysical driving force of transpiration, thereby contributing towards increasing transpiration rates, while partial stomatal closure under elevated [CO$_2$] will restrict the diffusion of water vapour out of leaves and act as a restraint on transpiration rates.

For example, previous calculations of transpiration rates from tree canopies showed that decreasing stomatal conductance by 10% would be sufficient to negate the effect of warming by 1 °C [13]. These two key opposing forces are thus of comparable magnitude. The key question is whether the balance of effects ultimately leads to increasing or decreasing transpiration rates. A number of studies have predicted that future evapotranspiration rates will increase substantially and could exceed increases in precipitation rates [e.g. 19–22], while other work suggested that future precipitation changes could exceed increases in transpiration rates [e.g. 13, 23].

Studies that have used and/or compared different approaches to calculate evapotranspiration rates showed that these different outcomes are sensitive to the choice of the equations that were used [e.g. 15, 24, 25•]. Studies based on the Thornthwaite method or derived equations, like the Palmer Drought Index, generally predicted large increases in evapotranspiration rates [e.g. 21, 22, 26], while studies based on more mechanistic approaches, like the Penman-Monteith equation, especially when they incorporated some degree of stomatal closure, predicted lesser or no future increases in evapotranspiration rates [e.g. 13, 23].

Here, we examine likely net changes in transpiration rates into the future. In particular, we aim to quantify the competing effects of temperature increases and stomatal closure. We use a mechanistic formulation for our calculations that explicitly includes each of the relevant factors and their changes. The analysis that follows is specific to the transpiration component of evapotranspiration.

What we describe could more strictly be described as potential transpiration or the transpiration rate controlled by plant and weather factors but assuming that there are no limitations by available water. In regions with severely limiting precipitation, transpiration rates will be determined by the amount of available water. Instantaneous weather factors are then relegated to secondary importance and plant factors are dominated by a response to available soil water. The work described here assumes no water limitations, or a prescribed stress level for the first and simplest case we explore, and then models the response of transpiration rate to other factors expected to change into the future.

It is based on a small set of key assumptions that include:

1. The transpiration rate of plant canopies can be calculated with the Penman-Monteith equation (PMeq).
2. The PMeq can appropriately include the effect of increasing temperature on ET, both directly and indirectly through changes in VPD.

3. Changes in VPD can be calculated based on the assumption that the diurnal temperature range does not change [13].

4. Decreasing stomatal conductance under elevated [CO_2] can be included in the PMeq by assuming that changes in canopy conductance are proportional to changes in stomatal conductance.

5. Stomatal conductance decreases under elevated [CO_2] to maintain a constant ratio of intercellular (c_i) to ambient (c_a) [CO_2].

6. Two extreme cases of photosynthetic responses to [CO_2] can be distinguished:

     a. Photosynthesis increases with increasing [CO_2] in accordance with photosynthetic theory (i.e. based on [27]).

     b. Photosynthetic downward acclimation negates any photosynthetic response to [CO_2] so that photosynthesis remains the same in low and high [CO_2].

In both cases, we assumed that a constant c_i/c_a is maintained. We excluded any changes due to changes in species shifts, canopy structure or nutrient feedbacks. We recognise that such other factors could play important additional roles, but the present work restricted itself to the defined smaller sub-set of possible interacting processes.

The validity of these various assumptions and their consequences is discussed and evaluated in the following. This is followed by the presentation of modelled results based on combining these assumptions.

Empirical Evidence to Underpin the Key Assumptions

Our calculations of changes in transpiration rates are based on the key assumptions stated above. In this section, we provide empirical evidence from the scientific literature to test these assumptions.

Calculating ET

Evapotranspiration rates can be calculated with a variety of different functions with different extents of physical rationales [28]. They range from very empirical, such as the Thornthwaite method [29], to strongly process-based formulations, such as the Penman-Monteith equation [30].

The Penman-Monteith equation is generally regarded as the best mechanistically based equation to calculate evapotranspiration rates [14, 15], and it has become the recommended standard formulation for calculating evapotranspiration rates in the field [31]. One of the important attributes of the Penman-Monteith equation is its explicit inclusion of stomatal

conductance to account for this important plant physiological response to an assessment of future water loss from plant canopies.

Stomatal Responses to Elevated [CO_2]

Experimental Observations

Increased [CO_2] generally leads to some stomatal closure in most plants. This has been observed in small-scale studies of both woody and herbaceous species. Various data compilations have shown that stomatal conductance is typically reduced by about 40% under doubled [CO_2] [32–36]. However, the extent of stomatal closure in woody species is generally smaller than in herbaceous species, with only 11–21% stomatal closure across a range of studies on woody species, with a weaker response in older than younger trees and a weaker response in conifers than deciduous trees [37, 38].

Importantly, changes in stomatal conductance are usually related to changes in assimilation rates so that the ratio of intercellular to ambient [CO_2] remains unchanged under elevated CO_2 [5]. This is a robust finding that allows some of the most confident predictions of future plant responses. Specifically, Medlyn et al. [37] found that future stomatal conductance could be modelled by fitting the Ball-Berry [39] model to available data from high-[CO_2] experiments. It implied that the functional relationship between photosynthesis and stomatal conductance is not altered by growth in elevated [CO_2].

In the Ball-Berry model, stomatal conductance is described explicitly as a function of [CO_2] and photosynthetic rate. If that relationship continues to hold across a wide range of [CO_2], it can greatly constrain possible future changes in stomatal conductance and water relations of plant canopies. Since the short-term response of photosynthesis to elevated [CO_2] is well understood, the key uncertainty thus relates to the extent of a possible long-term downward acclimation of photosynthesis to growth in elevated [CO_2] (as discussed further below). The possibility of downward acclimation means that there may be moderate stomatal closure if photosynthesis increases with increasing [CO_2] or even stronger stomatal closure if feedback processes prevent increases in photosynthesis under elevated [CO_2]. Both cases are explored in the following.

Historical Observations

As atmospheric [CO_2] has increased strongly over the past 100 years from a pre-industrial concentration of about 280 ppm to the recent 400 ppm, it is possible to observe realised stomatal responses to these natural changes in [CO_2] through direct or relevant proxy measures. A correlation

between [CO$_2$] and the number of stomata on leaves has been observed for plants grown under artificially altered [CO$_2$] [40]. The same correlation has been shown for herbarium specimens collected under different historical [CO$_2$] [41, 42], and even for specimens preserved in archaeological deposits [43]. While it is difficult to quantify these observations in terms of changes in stomatal conductance, it does show that stomatal responses to natural variations in [CO$_2$] are ubiquitous and persist even in plants exposed to elevated [CO$_2$] over extended periods.

Carbon Isotope Discrimination

The carbon isotope discrimination between $^{13}CO_2$ and $^{12}CO_2$ can also be used to infer changes in the ratio of intercellular to atmospheric [CO$_2$] [44] which can be related to historical changes in atmospheric [CO$_2$] [45]. Using this approach, various studies inferred reduced stomatal conductance in response to increasing atmospheric [CO$_2$] [46–49], although some other studies did not find similar evidence of stomatal closure in their data sets [50, 51].

More recently, studies of carbon isotope discrimination have been combined with evidence from eddy covariance data that allowed inference of water use efficiency from direct gas exchange measurements over successive years [52••]. Together, the combined data sets have provided strong support for the hypothesised increase in water use efficiency with increasing [CO$_2$] [3, 53, 54].

Historical River Runoff

Different studies have compiled data of global precipitation and river runoff [9, 55] and have shown that, despite decreasing precipitation, river runoff has increased since 1900 [9] and especially since 1960 [55]. Possible reasons include changes in land use, climate and the CO$_2$ and aerosol concentrations in the atmosphere. By modelling the influence of each of those factors separately for the five major continents and the world as a whole, it was found that the observed patterns were most consistent with a reduction in water use through stomatal closure in response to increasing [CO$_2$] [55].

Another study [56] has argued, however, that the transpiration-suppressing effect of [CO$_2$] would be negated through the greater leaf area that can develop through CO$_2$-enhanced growth. When that additional factor was included in their modelling, they concluded that overall, [CO$_2$] should have little net effect in reducing transpiration rates [56]. This study thus accepted that [CO$_2$] could lead to stomatal closure, but suggested that another CO$_2$-induced physiological factor, increasing leaf area, could have an effect on transpiration rates of similar magnitude but opposite sign.

Satellite Observations

Global satellite coverage over recent decades has given unprecedented and global coverage of any changes in foliage cover over time. These observations have generally reported greening of the globe [e.g. 57–59], but with simultaneous changes in the various underlying physiological drivers, it is not easy to unequivocally deduce the cause responsible for observed changes. Different equally valid analyses of the same underlying observations can then result in divergent conclusions [e.g. 58].

Donohue et al. [60••] tried to overcome some of the confounding factors by specifically focusing on observed trends in foliage cover in warm and dry environments. These are regions where temperature changes should play no significant role but where rainfall and [CO$_2$] would be the primary factors to control growth and foliage cover. They then showed that rainfall-use efficiency in the water-limited range of observation increased by about 11% between 1983 and 2010, which was attributed to increasing water use efficiency under elevated [CO$_2$] [60••].

Growth Experiments

For plant growth under elevated [CO$_2$], the critical question is whether plants under water-limed conditions show greater relative responses to CO$_2$ enrichment than plants grown with adequate water. In essence, if plants have access to a limiting amount of water, plant growth is determined by the amount of available water multiplied by the efficiency with which plants can use that water. Since water use efficiency under elevated [CO$_2$] is enhanced by both increases in photosynthetic rates and stomatal closure, it is numerically greater than the response of photosynthesis alone. That means that the relative growth stimulation by elevated [CO$_2$] should be greater under water-limited conditions unless it is over-ridden by additional higher-order plant physiological feedback processes.

Small-Scale Growth Experiments

A number of researchers have conducted high-CO$_2$ experiments with different levels of water availability and were able to compare plant growth responses between well-watered and water-stressed plants. For example, when different species were grown in wet and dry soils, it was observed that soil water was conserved under elevated [CO$_2$] and that water use efficiency greatly increased under both well-watered and water-stressed conditions [61, 62]. When these and similar findings were summarised, it was found that high-[CO$_2$] experiments commonly led to increased water use efficiency, but that plant water loss was not necessarily reduced because high-[CO$_2$] grown plants often had higher leaf areas [63].

One of the problems with the findings from small-scale growth experiments is the confounding effect of measurements during the plants' exponential growth phase which compounds initial direct CO_2 responses to greater ultimate growth responses. When results from published growth experiment were reanalysed by removing the confounding effect of measurements during the plants' exponential growth phase, it was found that the growth stimulation by elevated $[CO_2]$ was substantially greater under water-limited than well-watered conditions [6••].

Free-Air CO₂ Enrichment Experiments

A large review of Free-Air CO_2 Enrichment (FACE) recorded average increases in photosynthesis of about 30% and reduced stomatal conductance of about 20% for average $[CO_2]$ increases by about 200 ppmv [64]. In this compilation, tree species had particularly large photosynthetic increases, while reductions in stomatal conductance were more similar to that of other plant functional types. These average responses were in line with theoretical expectations.

Other analyses focused on the difference in growth response to elevated $[CO_2]$ between wet and dry conditions and showed the expected enhanced CO_2 response for grasslands, with relative growth responses being much greater under lower rainfall [65]. For C_3 crop plants, however, the growth enhancement by elevated CO_2 was only slight and not statistically significant [66].

Most FACE studies have also reported reductions in evapotranspiration rates [67]. However, a summary of results from existing FACE experiments from forests and other vegetation types did not find the expected enhanced growth stimulation under water-limited conditions, especially not in desert systems, for which a particularly strong water $\times$ CO_2 interaction might have been expected [68]. For forest systems, the data showed a slight decrease in CO_2 responsiveness with increasing mean annual rainfall, but when growth responses were calculated for each year separately, the driest years even had the weakest relative growth response to elevated $[CO_2]$ [68].

When the results of the Duke FACE experiment were analysed in greater detail, it was found that CO_2 responsiveness interacted with the stand's water and nutrient status [69]. Once the effect of nutrient status had been factored out, the expected enhanced relative growth stimulation at lower water availability emerged. The reconciled findings at the Duke FACE study highlight the difficulty of analysing the results of any specific study. Plants are always impacted by multiple internal and external factors that together determine their response to factors such as elevated $[CO_2]$. That also affects the interaction between the CO_2 response and factors such as the degree of water limitation. Without adequate consideration of these other factors, similar experimental conditions can lead to apparently divergent findings from similar experimental conditions and hinder the deduction of generic response patterns.

Acclimation of Photosynthetic Responses to Elevated [CO₂]

When plants are transferred to elevated $[CO_2]$, one can readily observe an immediate strong increase in photosynthesis. However, many studies have observed some degree of subsequent down-regulation of photosynthesis [67, 68, 70–73]. Arp [74] showed in a literature review that the extent of such down-regulation was strongly linked to the size of growth containers used, with strong down-regulation in small pots but no apparent down-regulations in field-grown plants. It pointed to an important role for root growth in utilising any extra available photosynthate under elevated $[CO_2]$. When root growth was curtailed by container size, it created a feedback inhibition that prevented the full utilisation of the potential CO_2 stimulation of photosynthesis.

A review of FACE experiments showed that down-regulation was also seen in many FACE experiments and was strongly correlated with changes in leaf nitrogen concentrations [68]. That suggested that even without root restrictions photosynthetic down-regulation could occur through a link with plants' access to nutrient resources. Most studies have reported decreasing soil nitrogen concentrations under high-$[CO_2]$ grown plants [75, 76]. Consistent with changes in soil-nutrient availability, plants grown in elevated $[CO_2]$ typically have lower nutrient concentrations, which has led to the general notion of progressive nitrogen limitation [69] that would curtail plant responses to elevated $[CO_2]$ [e.g. 77].

It is thus not clear to what extent future photosynthetic CO_2 assimilation rates will increase in line with predictions from photosynthetic theory [27] or whether actual changes in photosynthesis will be curtailed through downward acclimation. In the following, we have considered responses of transpiration to future climate and CO_2 concentrations under two scenarios: first, we assumed that photosynthesis would be enhanced by elevated $[CO_2]$, and second, we assumed photosynthesis would fully acclimate to increasing $[CO_2]$ such that photosynthesis remains the same as in the current climate.

Calculating Transpiration Rates

For the work described here, we used the PMeq to calculate transpiration rates [e.g. 14]. Details of the equation and its standard parameters are given in Appendix A. Here in the main text, we only describe those parts in greater detail that are important for determining its response to climate change.

The VPD, Δ, was calculated as:

$$\Delta = e(T_{day}) - e(T_{min}) \tag{1}$$

where the function $e(T)$ describes the saturation vapour pressure (in Pa) at a temperature T (°C), T_{day} is the daytime temperature at which calculations are done, and T_{min} is the overnight minimum temperature or some other minimum temperature that last condensed water and determined the vapour pressure in the present parcel of air. The diurnal temperature range was assumed to remain constant under climate change so that T_{day} and T_{min} were changed by the same amount in the simulations below (see [78] for simulations where the effects of that assumption were explored).

Aerodynamic resistance was treated as a constant for given vegetation types, thus ignoring any possible changes in wind profiles or canopy properties under future conditions. Canopy conductance was either treated as a constant for canopies under given physiological conditions (stressed or unstressed) as explicitly stated in respective sections below, or taken to be proportional to stomatal conductance, which was calculated based on the Ball-Berry relationship [39]. This ensured that a clear and explicit linkage between carbon gain and water use was maintained.

Stomatal conductance (mol m^{-2} s^{-1}) was therefore calculated as:

$$g_s = k A_n r_h / c_a, \qquad (2)$$

where k is a species-specific constant, A_n (μmol m^{-2} s^{-1}) is photosynthetic net assimilation rate, r_h is relative humidity (dimensionless), and c_a (ppm) is the surface [CO$_2$].

Two cases can be distinguished here: (1) assimilation rate increases in line with increases in intercellular [CO$_2$] and (2) photosynthetic downward acclimation forces A_n to remain the same in high and low [CO$_2$].

If A_n remains the same, and if k and r_h also remain constant, as was assumed here, then g_s simply scales inversely with c_a (Eq. 2).

If A_n increases with increasing [CO$_2$], it becomes necessary to calculate A_n, which, in turn, depends on the intercellular [CO$_2$], c_i. Since assimilation rate must also satisfy the general diffusion equation,

$$A_n = g_s (c_a - c_i)/1.6 \qquad (3)$$

with variables that have been defined before and the constant 1.6 that gives the ratio of the conductances of water vapour and CO$_2$ through the stomatal cavity.

Equations 2 and 3 can then be combined and rearranged to give:

$$c_i/c_a = \left[1 - \frac{1.6}{k r_h} \right] \qquad (4)$$

or

$$c_i = c_a \left[1 - \frac{1.6}{k r_h} \right] \qquad (5)$$

Equation 4 implies that the ratio of intercellular to ambient [CO$_2$] remains constant under elevated [CO$_2$] (see Stomatal Responses to Elevated [CO$_2$] Section), provided that relative humidity also remains constant. Using c_i calculated from Eq. 5, assimilation rates under different [CO$_2$] can then be calculated as described in Appendix A. Using Eq. 2, g_s can then be calculated from assimilation rates under different [CO$_2$].

For calculating changes in annual transpiration rates, we assumed that there would be no plant growth and no transpiration when monthly mean minimum temperatures were less than 0 °C [79]. Further details on the conversion from leaf level stomatal conductance to canopy conductance are given in Appendix A.

The non-linearity of the PMeq prompted us to check how changes in instantaneous calculations at single points in time relate to changes in mean daily transpiration rates. The advantage of reporting changes in instantaneous rates lies in its transparency. All relevant inputs are clear and involve just a single set of calculations. On the other hand, future changes in whole-day transpiration rates are generally more practically meaningful measures of water dynamics, but they involve many additional calculations. These complications can be avoided if relative changes of instantaneous and daily rates are the same.

We therefore tested how changes in instantaneous rates compared with changes in daily sums. Most of the inputs to the PMeq have large diurnal variations, especially when they include calculations of assimilation rates for calculating stomatal conductance. The non-linear interactions between these input variables could potentially mean that daily averages might respond differently to increased temperatures and [CO$_2$] than single-point calculations. Details of our test conditions and results are given in Appendix B.

The tests showed that the calculation of both instantaneous and daily transpiration rates increased similarly with increasing temperature by about 4% °C, with a similar temperature response over the entire CO$_2$ range (Fig. 10). Transpiration rates decreased by about 30% over the CO$_2$ range from 400 to 900 ppm. There was little difference between the temperature responses of instantaneous and daily transpiration rates, but in response to increasing [CO$_2$], instantaneous responses were about 10% larger than daily averaged responses. It was clear that for both instantaneous and daily-summed values, and across the range of potential future changes, the CO$_2$-driven reductions in stomatal conductance could have a greater effect on transpiration rates than the temperature- and VPD-driven increases. Both instantaneous calculations and calculations summed over whole days thus provided qualitatively similar answers that only differed marginally in their magnitudes. In the interest of maintaining transparency, we therefore opted to express results in the following based on instantaneous calculations.

Transpiration Rates Under Changing [CO₂] and Temperature

In the following, we illustrate the response of plant transpiration rates to changes in [CO₂] and temperature. Our main focus is on the response of forests in different regions of the world to expected changes over the twenty-first century. We begin by showing responses under standardised conditions and then move on to calculate responses based on expected changes in the key underlying drivers.

We used the PMeq to calculate changes in transpiration rate in response to changes in the underlying biophysical drivers (i.e. temperature and associated VPDs) and stomatal conductance. Transpiration rates increase strongly with increasing temperature (Fig. 1a), especially for unstressed forests, for which transpiration rates[1] increase from about 4 to 11 mmol m⁻² s⁻¹ from 5 to 40 °C.

Reducing stomatal conductance (in response to plant stress) reduces transpiration rates, especially for forests. At 5 °C, reducing stomatal conductance (to ¼) reduces forest transpiration rates by more than half, which is less evident in grasslands (Fig. 1b). In unstressed forests, transpiration rates increase with increasing temperature by about 4.5% °C⁻¹ (Fig. 1c). Proportionately, increases are less pronounced at higher temperatures, with increases in transpiration by unstressed forest increasing by only about 1.5% °C⁻¹ at 40 °C. Proportional increases are greater for stressed than unstressed stands. This is because with increasing transpiration rates, aerodynamic resistance attains increasingly greater importance and eventually curtails maximum rates, leading to diminishing responsiveness to increasing temperatures. Under stressed conditions, transpiration rates are less affected by these additional limitations.

Relative increases in transpiration rates with temperature are generally greater at lower temperatures, slightly greater for forests than for grasslands and greater under stressed than unstressed conditions (Fig. 1c, d). These temperature sensitivities are the basic measures that matter in assessing the response to climate change.

Figure 2 shows changes in transpiration rates for a range of possible combinations of increasing temperature and decreasing stomatal conductance. Relative changes in response to changes in the key drivers are numerically greater for forests (Fig. 2a) than grasslands (Fig. 2b), especially for the response of transpiration rates to stomatal closure. In essence, transpiration rates from forest canopies are predominantly controlled by VPDs, whereas transpiration rates from grassland canopies are more strongly controlled by radiation absorption [81].

Fig. 1 Calculated transpiration rates as a function of daytime air temperature (**a**, **b**) and their relative slopes, i.e. the percentage change in transpiration rate with increasing temperature (**c**, **d**). This is calculated for typical forests (**a**, **c**) and grasslands (**b**, **d**) that are either stressed or well-watered, with corresponding differences in canopy conductances. We assumed aerodynamic conductances of 3.33 cm s⁻¹ for forests and 1.54 cm s⁻¹ for grasslands [80] and canopy resistances of 2 and 0.5 cm s⁻¹ for unstressed and stressed plants, respectively. Net radiation was kept at 400 μmol (quanta) m⁻² s⁻¹ for all simulations, and the daytime minus night-time temperature difference was 10 °C

Increasing temperature and VPD therefore have stronger effects on forest than grassland transpiration. Through stomatal

Fig. 2 Relative change in transpiration rate for different combinations of increasing temperature and decreasing stomatal conductance, calculated for typical unstressed forests (**a**) and grasslands (**b**) at a daytime temperature of 20 °C

---

[1] For comparison, a transpiration flux of 5 mmol m⁻² s⁻¹, sustained over about half a day (i.e. 40,000 s), equates to a water loss of 3.6 kg m⁻² day⁻¹ or 3.6 mm day⁻¹.
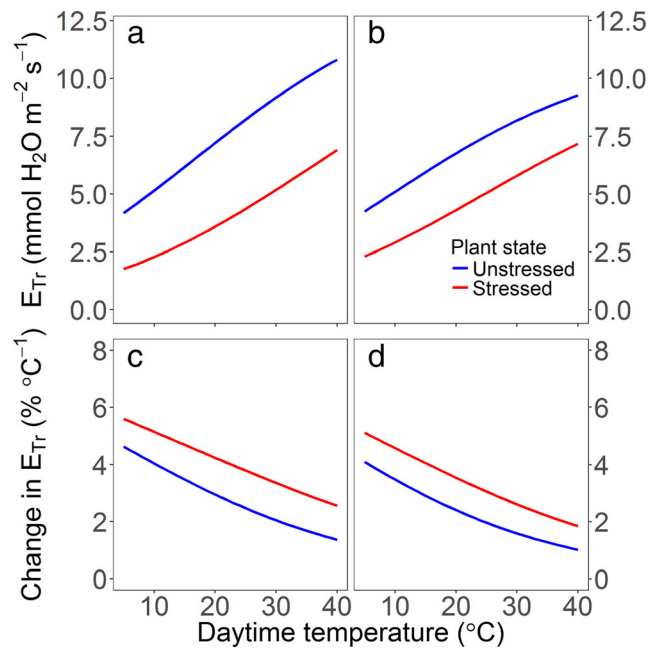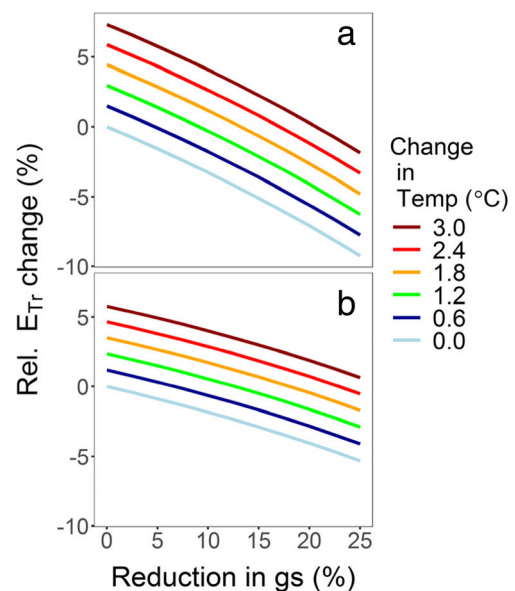
closure, forests can also exert greater control over their transpiration rates than grasslands. If grasslands partially close their stomata, the canopy's temperature increases, with the resultant increase in VPD largely negating the effect of stomatal closure. In better ventilated forest canopies, foliage heating is less pronounced through sensible heat exchange with the surrounding air so that a similar extent of stomatal closure can more effectively curtail transpirational water loss than in grasslands.

Having recognised that two facets of climate change—increasing temperature and rising $[CO_2]$—have opposing effects on transpiration, it is compelling to ask which process dominates. However, before we compare the importance of these opposing processes, we must consider the effect of an additional feedback effect. Any $[CO_2]$-stimulated increases in photosynthesis are likely to also increase leaf area. This creates a positive feedback to stimulate photosynthesis even more through enhanced radiation absorption. More radiation absorption by greater leaf area will also increase transpiration rates. While increasing $[CO_2]$ reduces transpiration rates through stomatal closure, any attendant increases in photosynthesis also act to increase transpiration rate by maintaining higher stomatal conductance and providing enhanced leaf area for radiation absorption.

The extent of this additional effect is illustrated in Fig. 3a by showing future photosynthesis rates under expected $[CO_2]$ with and without the leaf area feedbacks (Fig. 3b). If LAI is kept constant, relative plant responses to increasing $[CO_2]$ are the same irrespective of their LAIs (the solid lines in Fig. 3a). However, if changes of increasing leaf area are included, it further enhances the direct photosynthetic response (dashed lines).

This is most pronounced for plants with low initial LAI at low $[CO_2]$, for which the response to elevated $[CO_2]$ can be increased substantially through the LAI feedback. With increasing initial LAI, the importance of that feedback effect diminishes as most radiation can be absorbed even by the lower initial leaf area. While leaf area still increases with further increasing $[CO_2]$, it is physiologically less significant because it provides little additional radiation absorption, with the consequent positive feedback effect being muted.

The simulations in the rest of the paper used an LAI/A_n ratio of 0.2, a value appropriate for relatively dense initial canopies (LAI ≈ 4). Calculated changes in transpiration rates with increasing $[CO_2]$ and warming thus essentially compare the effectiveness of transpiration-suppressing stomatal closure with transpiration-enhancing increasing temperature. The positive feedback effect of enhanced leaf area development contributes towards increasing future transpiration rates. This feedback effect would have been more pronounced if parameters with lower initial LAI had been used and less pronounced if higher initial LAI had been simulated.
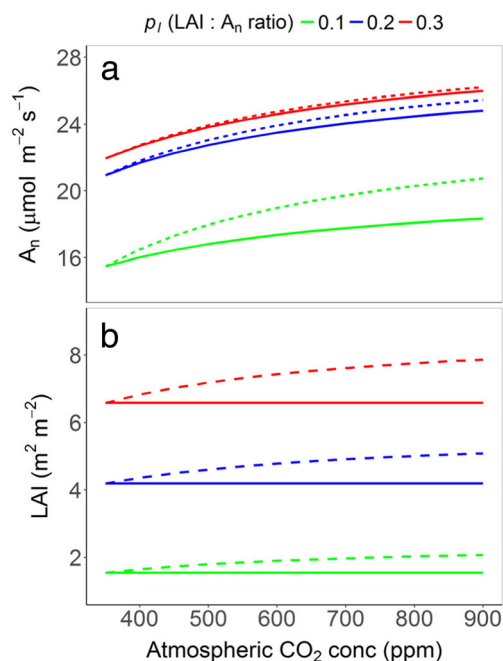
Fig. 3 Photosynthetic rate (A_n) and leaf area index (LAI) in response to increasing atmospheric $[CO_2]$. The solid lines indicate simulations without including a feedback response between A_n and LAI (solid lines). The dashed lines show simulations with an assumed feedback that is driven by a constant proportionality between A_n and LAI and a Beer's Law dependence of absorbed radiation on LAI. The different line colours indicate simulations with three possible values of the proportionality constant p_l (the LAI/A_n ratio)

Figure 4 shows the response of transpiration rates to changes in atmospheric $[CO_2]$ for forests and grasslands at different daytime temperatures mediated through stomatal closure in response to increasing $[CO_2]$. Over the range of $[CO_2]$ from the concentration of 350 ppm in the 1980s to possible 2100 values of 900 ppm, stomatal conductance is expected to decrease by about 60%, leading to an approximate reduction in transpiration rates in forests by 37–44% (at different temperatures) when LAI was kept constant and by 34–43% with inclusion of LAI feedbacks. While the absolute effect of the LAI/A_n feedback on E_{Tr} is only minor, it has been included in all subsequent calculations.

In contrast to the response of forest systems, transpiration rates from grasslands are less responsive to stomatal closure with reductions in transpiration rates by 26–35% (with LAI feedbacks). As stated before, transpiration rates from grasslands are more strongly controlled by radiation than transpiration rates from forests. That means that other factors, such as temperature, VPD or stomatal conductance, have greater influence on forest than grassland transpiration.

Figure 5 shows calculations for one specific climate change scenario for a New Zealand forest, with changes in the key quantities over time. It uses the same assumptions regarding aerodynamic resistance of forest ecosystems as given in
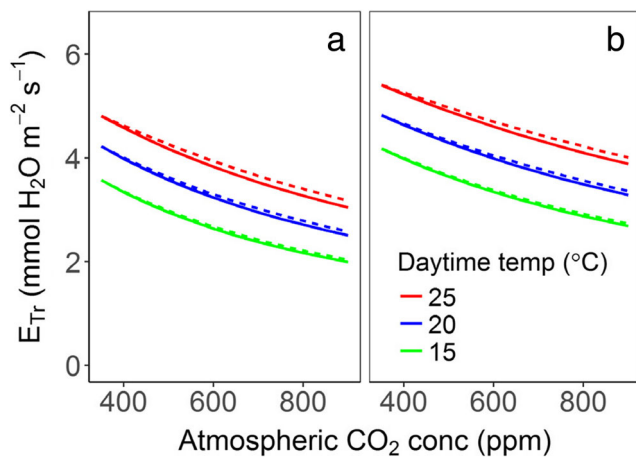
Fig. 4 Calculated transpiration rates for forests (**a**) and grasslands (**b**) in response to changes in stomatal conductance resulting from changes in atmospheric [CO_2] as shown in the figure. This is shown for three different daytime temperatures. Dashed lines show simulations with inclusion of the LAI/A_n feedback, whereas simulations with constant LAI are shown by the solid lines. Modelling details are given in Appendix A

Fig. 4a). These calculations are done under three representative concentration pathways [11]. RCP 2.6 represents an optimistic sustainable future scenario, with [CO_2] peaking in the middle of the twenty-first century, while RCP 6.0 represents a more realistic high-emission scenario and RCP 8.5 represents a scenario with even higher emissions and consequent atmospheric [CO_2] (Fig. 5b). A fourth frequently used RCP, RCP 4.5, showed modelled responses that were generally similar to those under RCP 6.0. In the interest of clarity, these simulation results have been omitted from the following graphs.

Temperature is expected to increase strongly over the twenty-first century, especially under RCP 8.5 (Fig. 5a). Expected increases are more moderate under RCP 6.0, and under RCP 2.6, temperatures may even peak by about 2060 with little consistent pattern thereafter. These temperature increases are associated with increasing VPDs that may increase by as much as 25% under RCP 8.5, with more moderate increases under RCP 6.0 and increases of only about 5% under RCP 2.6 (Fig. 5c).

These temperature increases are largely driven by increases in [CO_2] that could reach concentrations of over 900 ppm by the end of the century under RCP 8.5 (Fig. 5b). Increasing [CO_2] not only adds to global warming but also allows greater photosynthesis. Under RCPs 6.0 and 8.5, assimilation rates are projected to increase steadily throughout the twenty-first century, but under RCP 2.6, they are expected to increase only to about 2040 before returning to values similar to those in the twentieth century (Fig. 5d). Even though the [CO_2] responsiveness of photosynthesis decreases under higher [CO_2], under RCP 8.5, this is negated by the accelerating rates of increase in atmospheric [CO_2] to lead to the calculated ongoing increases in photosynthesis. These increases in [CO_2] also cause stomatal conductance to decrease sharply. Although increasing assimilation rate acts as one factor to maintain higher stomatal conductance, a direct response to increasing [CO_2] has an overriding effect, and under RCP 8.5, stomatal conductance is expected to be more than halved by the end of the century (Fig. 5e).

Fig. 5 Anticipated future conditions for at a site in the Bay of Plenty region in New Zealand (Table 1). Shown are mean temperatures (**a**), corresponding changes in atmospheric [CO_2] (**b**), relative change in calculated VPDs (**c**), rate of photosynthesis (**d**), relative change in stomatal conductance (**e**) and relative change in canopy transpiration rates (**f**) over the twenty-first century, calculated under three different RCPs as shown in the figure. Quantities in **c**, **e** and **f** have been expressed as deviations from their respective 1980 values
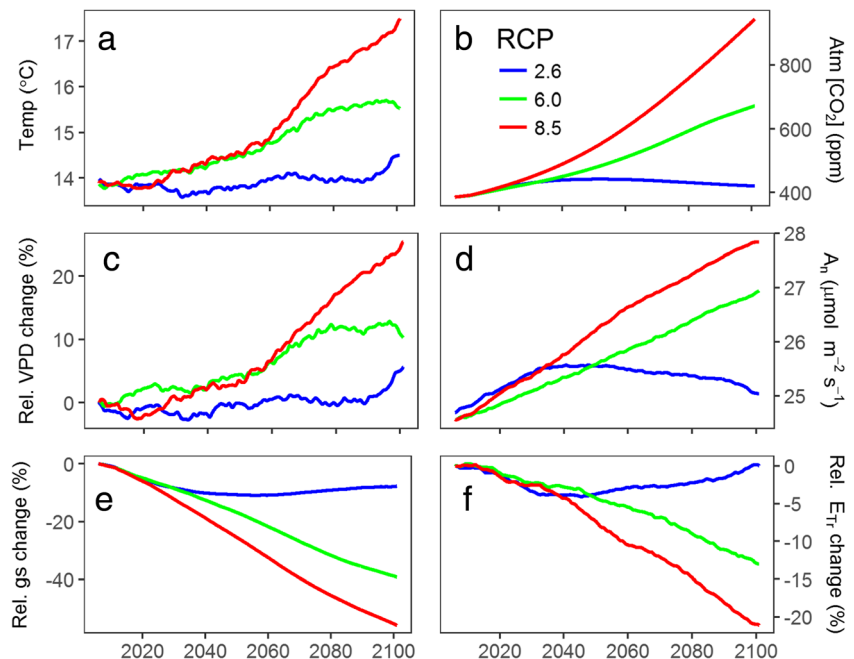
This provides both positive and negative effects on transpiration rates, but with all factors combined, they point towards reducing transpiration rates (Fig. 5f). Projected changes are quite strong under RCP 8.5, with transpiration rates reduced by more than 20% by the end of the century. This net reduction in transpiration rates shows that strongly reduced stomatal conductance in response to a large relative increase in $[CO_2]$ is the dominant influence on future transpiration rates. Reductions in transpiration rates are greatest under the highest RCP. Reductions in transpiration rate are also apparent and reasonably strong under RCP 6.0, but under RCP 2.6, transpiration rates at the end of the century are essentially the same as currently.

The reductions in transpiration rate shown in Fig. 5f have been calculated under the assumption that assimilation rate will increase in line with predictions based on the relevant photosynthetic theory (Fig. 5d). However, many experiments have found that photosynthetic responses to elevated $[CO_2]$ are sometimes only transitory (see Acclimation of Photosynthetic Responses to Elevated $[CO_2]$ Section) before returning to rates similar to those of plants in lower $[CO_2]$. We explore here how the uncertainty about photosynthetic responses would affect inferred changes in transpiration rate (Fig. 6).

The simulations show that transpiration rates will be reduced even more if photosynthesis does not increase under elevated $[CO_2]$ (dashed lines in Fig. 6a) than if photosynthesis increases (solid lines). These differences are also quite substantial, with reductions in transpiration rates amplified by about one third if there are no changes in assimilation rates. For plant growth, water use efficiency is ultimately the most important measure of future water limitations. Water use efficiency is also expected to increase substantially over the twenty-first century, with responses being reasonably insensitive to assumptions regarding photosynthetic downward acclimation (cf. the dashed and solid lines in Fig. 6b).

The comparison of Figs. 5d and 6b shows that there can be much greater gains in water use efficiency than in photosynthesis alone. The magnitude of growth gains under increased $[CO_2]$ thus depends on environmental conditions, especially the extent of water limitation. Relative gains under elevated $[CO_2]$ are likely to be greatest on water-limited sites where nutrition is adequate because that is where feedback inhibitions through nutrient depletion are minimised and where water use efficiency, rather than direct CO_2 responses of photosynthesis, attains its greatest importance [82, 83].

Changes in transpiration rates will depend strongly on the relative magnitudes of changes in $[CO_2]$ and temperature. CO_2 is a long-lived gas that is well-mixed in the atmosphere, leading to similar rates of increase across the globe. Concentration differences between sites can therefore generally be ignored. Temperature increases, however, are more variable, with greater increases at high latitudes, in particular, while smaller increases are generally expected for tropical regions or islands where temperature increases are likely to be buffered by the more-slowly warming oceans [1]. Even the same temperature changes can lead to different relative changes in transpiration rates as transpiration rates are proportionately more responsive to temperature changes at colder than warmer starting temperatures (see Fig. 1b).

In order to investigate how the opposing influences of $[CO_2]$ increases and warming will affect forest transpiration rates into the future, we obtained background climates and expected climatic changes for six representative sites across the globe. They range from tropical to boreal locations and cover both southern and northern hemispheres. Mean annual temperatures range from − 3 °C at the Canadian site to 27 °C in Brazil (Table 1).

The simulations show reductions in transpiration rates for most sites and most RCPs, with reductions increasing with higher RCPs (Fig. 7). Reductions in transpiration rates are even greater if there is photosynthetic downward acclimation (dashed lines). It indicates that the transpiration-depressing effect of elevated $[CO_2]$ generally dominates over the

Fig. 6 Calculated changes in transpiration rates (E_{Tr}) (a) and resultant water use efficiency (b) for forest canopies assuming that assimilation rates are increasing (solid line) or remain constant (dashed) due to photosynthetic downward acclimation. Simulations are shown under three RCPs as shown in the figure. The solid lines in a are the same data as shown in Fig. 5f
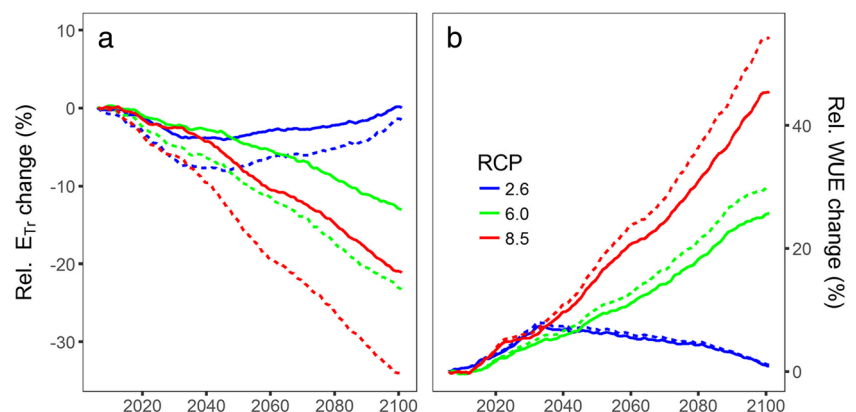
Table 1 Selected forest zones used for subsequent simulations and corresponding climatic data

Forest ecosystem	Climate	Site	Lat.	Long.	Annual mean temp. (°C)	Predicted temperature change from 2000 to 2100 (°C)		
						RCP		
						2.6	6.0	8.5
Temperate Forest, New Zealand	Temperate, oceanic	25 km NE of Rotorua, NZ	− 37.8°	176.3°	14	0.4	1.8	4.2
Temperate Forest, Australia	Temperate, continental	Armidale, NSW	− 30.4°	151.6°	13	2.0	2.1	3.6
Tropical Rainforest, Brazil	Tropical, moist	Manaus, Brazil	− 2.7°	− 68.4°	27	1.7	3.7	6.4
Boreal Taiga, Canada	Cool, dry	Thompson, Canada	55.7°	− 97.9°	− 3	3.7	4.8	6.3
Temperate Broadleaf	Temperate	Harvard Forest, MA, USA	42.5°	− 72.2°	8	2.0	3.1	6.7
Temperate evergreen conifer	Temperate	Tiveden, Sweden	58.7°	14.6°	11	2.0	3.7	4.0

Data sources are given in Appendix A

transpiration-enhancing effect of increasing temperature. The only site with only minor changes under any RCP is the tropical rainforest site in Brazil, where the stimulating and inhibiting processes had similar weight.

For all sites, there are only minor transpiration changes under RCP 2.6 — it even increases slightly (Fig. 7). Under RCP 2.6, highest [CO_2] is reached by the middle of the twenty-first century, with decreasing concentrations thereafter (Fig. 5b). Hence, the transpiration-depressing factor would be waning by the end of the century, while the transpiration-enhancing increased temperatures still persist to lead to slight increases in net transpiration rates.

This partly reflects the temporal disconnect between [CO_2] and subsequent climate change. Under the rapidly increasing [CO_2] under RCP 8.5, the transpiration-depressing effect is effective before the full warming is fully realised some decades later. Under RCP 2.6, [CO_2] increases first but then begins to fall in the latter parts of the twenty-first century. That gives time for the transpiration-enhancing warming to catch up, leading to gradually increasing transpiration rates over the latter part of the twenty-first century.

While instantaneous transpiration rates decrease under RCP 8.5, this can be negated by lengthening growing seasons for many locations around the world (Fig. 8). In Australia, New Zealand and Brazil, even current temperatures already allow year-round photosynthesis and transpirational water loss so that warming does not change the length of the growing season.

For colder sites with current growing seasons of less than 365 days, however, any future warming is likely to lengthen the growing season (Fig. 8b, d, f) and with it annual total transpiration rates [18]. At some sites, lengthening growing seasons can turn small changes in summertime transpiration rates into increases in total annual transpiration rates (Fig. 8a, c, e), especially where the fractional change in growing season length is quite large, such as at the taiga site (Fig. 8a, b).

Surprisingly, once changing season length is factored in, the largest increases in annual transpiration rates are seen under RCP 2.6 because even the small warming under RCP 2.6 can be appreciable but any transpiration-depressing increase in [CO_2] will have dissipated by the end of the twenty-first century. Consequently, while under RCP 2.6, there are expected to be only slight changes in instantaneous transpiration rates at the boreal site (Fig. 8a), increasing growing season lengths turn those into substantial season-long increases of about 35% (Fig. 8a). The enhancement of changes in seasonal transpiration compared to instantaneous rates is similar under the other RCPs.

For the taiga (Fig. 8b), and especially the temperate broadleaf forest site (Fig. 8d), the increase in growing season length can be substantial. Even though the expected warming is greater for the taiga than for the temperate broadleaf forest site (Table 1), its effect on growing season length is more pronounced for the temperate site. As current temperatures are already close to the defined productivity threshold, a given temperature increase can lead to a greater change in growing season length than for the taiga site with a more extreme current climate. On the other hand, even the smaller increase in growing season length at the taiga than the broadleaf site constitutes a greater relative increase, thus having a greater effect on percentage changes in transpiration rates.

Discussion

Our aim here was to explore the net effect of the interacting and opposing drivers of transpiration rates under future climatic conditions. In particular, we aimed to compare the relative effects of transpiration-enhancing temperature increases and transpiration-depressing [CO_2] increases. For that, we used the PMeq, a model for evapotranspiration that has been
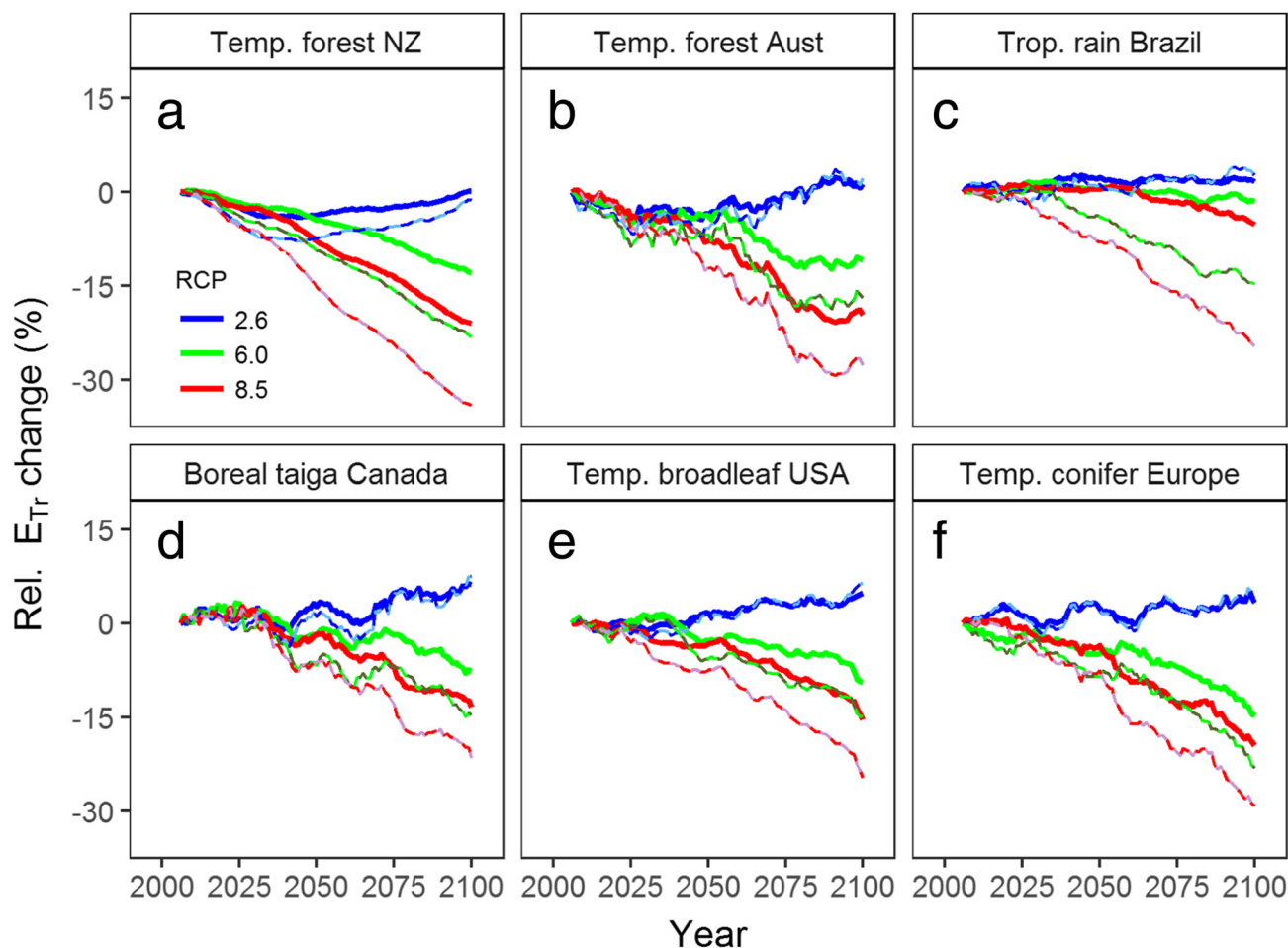
Fig. 7 Relative changes in transpiration rates under changing air temperatures and atmospheric $[CO_2]$ for forest canopies in six different regions of the world (Table 1). The solid lines indicate changes in daytime transpiration rates (averaged over the length of current-day growing seasons) calculated with inclusion of increasing photosynthesis. The narrow dashed lines give changes with full photosynthetic downward acclimation (no change in assimilation rate)

well validated since the 1960s and is widely used to simulate biophysical soil-plant-water relationships in many different surface vegetation models. The PMeq can be used to calculate transpiration or evaporation rates or estimate evaporation and transpiration concurrently [17•, 84, 85].

Mechanistic modelling of evapotranspiration rates can provide useful and reliable insights about future conditions provided that all relevant biophysical factors and their dynamics are represented realistically. The key inputs are the biophysical drivers of evapotranspiration, including temperature and vapour pressure deficit. In an assessment of future conditions, there are likely to be only small changes in net radiation. For estimating future transpiration rate, it is critically important to also consider likely changes in stomatal conductance [16•, 17•] and its linkage to photosynthetic rates. Finally, locations with lengthening growing seasons may have increasing annual sums of transpiration rates even if instantaneous summer rates do not change or decrease. For understanding the overall

balance of the water cycle, these rates of water loss must then be brought together with possible changes in precipitation.

Our analysis indicated that for most sites, reductions in stomatal conductance driven by increases in atmospheric $[CO_2]$ are likely to be of greater importance in determining changes in transpiration rates than increases in temperature and associated VPD. It largely supports the notion that there will be lower transpiration rates in the future and thus reduced water limitations for plant productivity, especially for forest systems. The water relations of plant canopies are one of the most important determinants of future plant productivity [e.g. 60••, 78, 86]. Water dynamics are also important on their own as determinants of downstream water flows [54, 55], which is important for the prediction of future water availability and infrastructure needs for the regulation of water flows [e.g. 87].

Our findings are largely consistent with most recent work [13–15, 23, 25•, 78, 86] but conflict with the findings of others, whose modelling work suggest a dominant drying
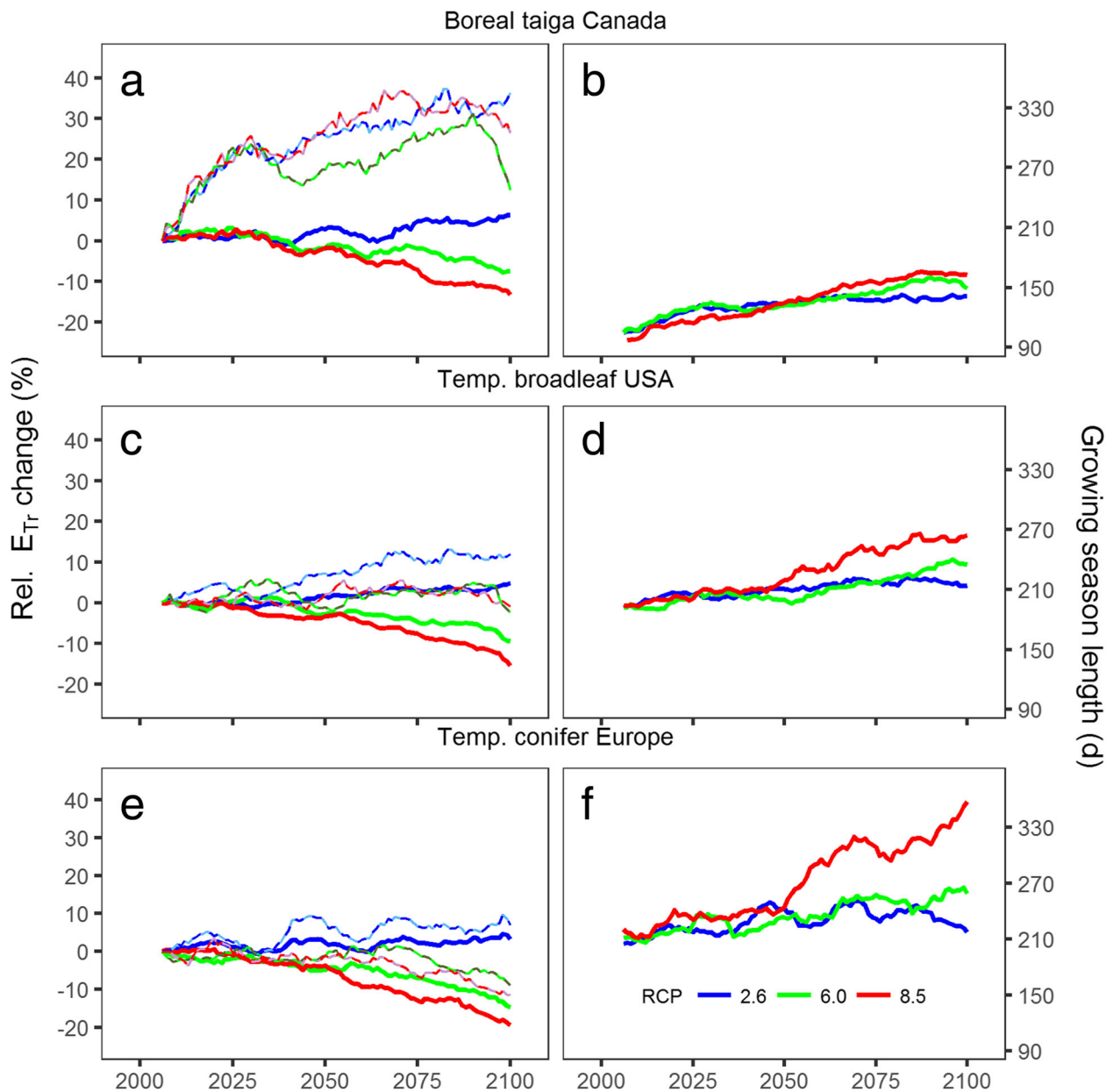
Fig. 8 Changes in relative transpiration rate, E_{Tr} (**a**, **c**, **e**), and calculated lengths of the growing seasons (**b**, **d**, **f**) for three forests subject to winter dormancy. Different colours represent the three different RCPs. In panels **a**, **c** and **e**, the lines indicate relative E_{Tr} changes calculated under changing air temperatures and atmospheric [CO_2] totals for unadjusted annual averages (thick lines, same as in Fig. 7) and for annual averages that have been adjusted to account for the lengthening growing season (narrow, dashed lines)

trend in future [19–22, 26, 88, 89]. As pointed out in the early work of McKenney and Rosenberg [15], there is a key difference between predictions based on mechanistically based models, like the Penman-Monteith equation, and simpler formulations, like the Thornthwaite method.

The Thornthwaite method [29] uses the current correlation between the key drivers of evaporation rates, temperature and radiation, to provide a simplified assessment of responses to future conditions. These simplifications, however, are not likely to hold in future as warming will not be accompanied by corresponding increases in net radiation. Enhancements of

evaporation rate based on the Thornthwaite method are therefore likely to significantly overestimate future increases in evaporation rates. Thus, only formulations that explicitly include all the different drivers of evaporation rates, and their projected changes into the future, can give balanced assessments of likely future evaporation rates [15, 25•].

Furthermore, for predicting changes in transpiration rather than evaporation rates, any changes in stomatal conductance also need to be explicitly included in the assessment [e.g. 13, 16•, 17•]. While many uncertainties remain in the response of plants to a changing climate, one of the most consistent

responses is partial stomatal closure in response to increasing [CO$_2$] (see the list of relevant observations given in Empirical Evidence to Underpin the Key Assumptions Section above). While evaporation rates are solely driven by physical weather factors, transpiration rates are additionally impacted by this direct plant physiological response to [CO$_2$]. For an overall assessment of future water balances, changes in both evaporation and transpiration are important. With transpiration rates becoming curtailed by partial stomatal closure, evaporation is therefore likely to become relatively more important as a process of water loss.

There are likely to be different patterns of changes in evaporation or transpiration rates across the globe (e.g. Figs. 6 and 7) [23, 90]. Our present work aimed to complement these global studies by focusing more strongly and explicitly on the interplay between the key driving variables that are generally not discernible within global-scale simulations. All sites experience similar changes in [CO$_2$], but even the physiological response to a given change in [CO$_2$] is likely to vary in conjunction with differences in background air temperatures. The CO$_2$ limitation of photosynthesis generally increases with increasing temperatures [27] so that the CO$_2$ responsiveness of photosynthesis is expected to be greater for sites from warmer than cooler locations.

While the direct effect of elevated [CO$_2$] in reducing stomatal conductance can have the same effect everywhere, the stimulation of photosynthesis is more important at warmer sites. Any stimulation of photosynthesis would act to keep stomata open under elevated [CO$_2$]. That effect can be seen in the difference between acclimated and non-acclimated simulations being largest for the tropical simulations and less pronounced for temperate and boreal forests (Fig. 7).

The transpiration-suppressing direct [CO$_2$] effect then competes with the transpiration-enhancing effect of increasing temperature and VPD. Among our investigated sites, temperature increases were particularly small for New Zealand (Table 1), probably because New Zealand is a relatively small island surrounded by ocean that buffers future temperature increases. With less temperature-driven enhancement of transpiration rate, the depressing effect of increases in [CO$_2$] dominates the overall response for a relatively large net reduction in transpiration rates (Fig. 7).

The high-latitude sites in Sweden and the taiga, in contrast, can expect higher temperature increases, with relatively little net change in transpiration rates over the summer months. Summed to a whole year, however, transpiration rates of these sites can increase substantially, especially that of the taiga site because of the effect of substantially lengthening growing seasons (Fig. 8).

In the present work, we have focussed solely on transpiration and the interplay between stomatal conductance and atmospheric evaporative demand, as forced by changes in temperature and VPD. In contrast to transpiration rates, evaporation rates will not be curtailed by changes in stomatal conductance and could respond solely to the transpiration-enhancing effect of increasing temperature. Evaporation rates from free surface water or moisture on soil surfaces may thus increase while plant transpiration rates will not. While total water dynamics from vegetated land surfaces are usually dominated by transpiration, a consideration of total water dynamics needs to consider both evaporation and transpiration fluxes together. The evaporation from wet canopies after rainfall events may be particularly important for dense canopies that rely on repeated replenishment of their water resources. If that is reduced through greater evaporation of water from the canopy it could critically reduce the replenishment of the water resources of those canopies.

Overall water balances will be affected by the combined effect of changes in both evaporation and transpiration rates. Enhanced evaporation rates will affect longer-term water balances by reducing soil water recharge when the canopy and soil are wet. As soils partially dry, evaporation rates diminish, water loss by transpiration begins to predominate and any reductions in transpiration rates may delay the onset of developing water stress.

Detailed assessment of changes in transpiration rates for a small number of specific sites also allows a detailed analysis of the importance of specific components of the overall response, such as the [CO$_2$] × temperature interaction in the photosynthetic response to elevated [CO$_2$]. This is clearly seen through the difference between acclimated and non-acclimated changes in transpiration rates. Where temperatures are high, as in tropical forest, the difference between acclimated and non-acclimated responses is larger than in Sweden or the taiga where temperatures are lower (Fig. 7). A strong [CO$_2$] × temperature interaction is deeply embedded in the relevant underlying photosynthetic equations.

However, as a further complication, when Kirschbaum and Lambie [6••] reviewed and reanalysed a large number of observations of growth responses to elevated [CO$_2$], they did not find the expected [CO$_2$] × temperature interaction. Instead, they found very little difference in growth responses to elevated [CO$_2$] across a wide range of temperatures [6••]. This has important implications for expected growth responses to naturally increasing [CO$_2$] for regions with different temperatures. This is an important current source of uncertainty that needs urgent resolution to provide more confident prediction of likely growth responses in the future.

The simulations shown here used a stand-level approach where conditions external to the stand were assumed to be unaffected by simulated changes within the stand. However, if whole landscapes respond similarly to an external factor, such as stomatal closure in response to elevated [CO$_2$], then larger scale feedback processes play an additional role [81]. In addition to radiative forcing by elevated [CO$_2$], partial

stomatal closure in response to elevated [CO_2] reduces transpirational surface cooling and thereby adds to global warming (termed 'CO$_2$ physiological forcing'). This CO_2 physiological forcing was calculated to add an additional 10–15% to global warming, especially over forested regions [91–93].

However, despite the reduced transpiration rates, studies using global circulation models generally found only small effects of CO_2 physiological forcing on atmospheric moisture levels, thus not contributing a further feedback effect. While reductions in atmospheric moisture levels might have been expected, there are complex reasons responsible for this absence of a relationship as discussed in detail by Boucher et al. [92].

Importantly, these global studies suggest that there are only minor landscape-level feedbacks between transpiration rates and the drivers of transpiration rates. They are largely restricted to a small additional temperature increase by CO_2 physiological forcing but are not further impacted by changes in atmospheric moisture levels. It means that the stand-level findings shown above are unlikely to be overturned by wider-system feedback effects.

Conclusions

In this work, we brought together a number of separate elements to calculate future transpiration rates. The calculation of transpiration rates is well supported by the relevant underlying theory, and the key assumptions are well supported by relevant empirical observations. Together, they point to reduced transpiration rates into the future for most parts of the world because for most locations and under most RCPs, stomatal closure under elevated [CO_2] has a quantitatively larger effect in reducing transpiration rates than the effect of increasing temperature in increasing transpiration rates.

Uncertainty remains in relation to the full extent of increases in photosynthesis under elevated [CO_2]. This leads to a range of possible reductions in transpiration rates from moderate if there is a strong increase in photosynthesis to even greater reductions in transpiration rates if photosynthetic rates remain similar to present-day rates. Calculated changes in water use efficiency were even greater than reductions in transpiration rates and attained similar values irrespective of the uncertainty around photosynthetic adjustments. In currently cold parts of the world, however, increases in instantaneous transpiration rates were partly negated through lengthening growing seasons so that transpirational water loss over a whole season were found to increase at some locations even though daily transpiration rates during their current growing season may decrease [e.g. 18].

The water relations of plant canopies are one of the most important determinants of future plant productivity.

Stand-level water dynamics are also important determinants of downstream water flows, which are important to predict future water availability and infrastructure needs for the regulation of water flows. It is, therefore, critically important to better understand any changes in these key fluxes. Through our work here, we aimed to contribute to a better understanding of likely future changes in these key processes. The work shows that alarmist negative outlooks are not warranted. Changes instead are likely to be complex and differentiated, depending in parts on factors such as possible photosynthetic downward acclimation and whether increases in season length may increase annual transpiration rates even if daily rates during current growing seasons may not change. A full assessment of future water dynamics requires a careful assessment of possible changes in their respective environments and individual circumstances.

Compliance with Ethical Standards

Conflict of Interest The authors have nothing to disclose.

Appendix A. Equations used for modelling transpiration rates

Calculating transpiration rates

For the work reported here, transpiration rate, E_{Tr}, was calculated with the Penman-Monteith equation [30] as:

$$E_{Tr} = \frac{\sigma Q_a + \Delta \rho_a C_p / r_a}{\sigma + \gamma (r_a + r_c)/r_a} / L_h \tag{A1a}$$

or

$$E_{Tr} = \frac{\sigma Q_a + \Delta \rho_a C_p g_a}{\sigma + \gamma \left({}^1/_{g_a} + {}^1/_{g_c} \right) g_a} / L_h, \tag{A1b}$$

where σ is the derivative of the saturation vapour pressure curve with respect to temperature, Q_a [W m^{-2}] is net radiation absorbed by the canopy, ρ_a the density of air, C_p the specific heat of air, Δ [Pa] the vapour pressure deficit of the air, γ the psychrometric constant, L_h the latent heat of vaporisation and

r_a and r_c are aerodynamic and canopy resistances. Equation A1b is the equivalence of Eq. A1a but uses aerodynamic (g_a) and canopy (g_c) conductances instead of resistances.

The vapour pressure saturation deficit was calculated as described in Section "Calculating Transpiration Rates" with

$$e(T) = 610.78 e^{17.269T/(T+237.3)} \quad [\text{Pa}]. \tag{A2}$$

The psychrometric constant, γ, scales linearly with atmospheric pressure. The other terms in Eq. A1 were treated as constants and small temperature dependencies [see 14] were ignored.

$$\sigma = 4098\Delta/sqr(T_{day} + 237.3) \quad [\text{Pa K}^{-1}] \tag{A3a}$$

$$L_h = 45 \quad [\text{kJ mol}^{-1}] \tag{A3b}$$

$$\rho_a = 0.02898 P_{atm}/(R\,T_K) \quad [\text{kg m}^{-3}] \tag{A3c}$$

$$C_p = 1.013 \quad [\text{kJ kg}^{-1}\text{K}^{-1}] \tag{A3d}$$

$$\gamma = 0.02898\,\rho_a P_{atm}/L_h \quad [\text{Pa K}^{-1}], \tag{A3e}$$

where T_{day} is the daytime temperature for which calculations are made, and P_{atm} is atmospheric pressure (in Pa).

The aerodynamic resistance, r_a, in Eq. A1a was set as a constant for general vegetation types. We used daily average values measured during mid-summer at a woodland and grassland site in California [80] of:

$$r_a = 30 \text{ s m}^{-1}\left(g_a = 3.33 \text{ cm s}^{-1}\right) \quad \text{for forests}; \tag{A4a}$$

$$r_a = 65 \text{ s m}^{-1}\left(g_a = 1.54 \text{ cm s}^{-1}\right) \quad \text{for grasslands}. \tag{A4b}$$

The canopy conductance, g_c, in Eq. A1 was either calculated explicitly from stomatal conductance in relation to photosynthetic carbon gain, as described below, or set to specific prescribed values for some generic illustrations to:

$$r_c = 50 \text{ s m}^{-1} \quad \left(g_c = 2 \text{ cm s}^{-1}\right) \quad \text{unstressed conditions}; \tag{A5a}$$

$$r_c = 200 \text{ s m}^{-1} \quad \left(g_c = 0.5 \text{ cm s}^{-1}\right) \quad \text{stressed conditions}. \tag{A5b}$$

In the explicit calculation based on calculated stomatal conductance, we calculated canopy conductance, g_c (in units of cm s^{-1}), from g_s and ρ_a:

$$g_c = 2.898\, g_s/\rho_a \tag{A6}$$

Calculating stomatal conductance and photosynthetic rates

We used the Ball-Berry equation [39] to calculate g_s as a function of assimilation, relative humidity and [CO_2] given

in Eq. 2 in the main text. The empirical parameter linking these quantities was set to 9 [94].

R_h is relative humidity, calculated simply as:

$$R_h = e_a/e_s \tag{A7}$$

where e_a is the vapour pressure of the bulk air and e_s is the saturated vapour pressure at leaf temperature.

For the present purpose, net assimilation rate A_n was calculated as the Ribulose-1,5-bisphosphate (RuBP) regeneration limited rate of photosynthesis [27, 94] as:

$$A_n = w_j, \tag{A8}$$

where w_j is the RuBP regeneration-limited rate. We chose to base our calculations on the RuBP-regeneration-limited rate as that is the relevant limitation under low light, thus for the majority of conditions during the day and for foliage partly shaded by other leaves in the canopy, under cooler conditions since RuBP regeneration tends to be more temperature sensitive than Rubisco-based photosynthesis [27, 95], and under higher [CO_2]. The RuBP-regeneration-limited rate is therefore likely to be the more common limitation, especially under future [CO_2]. It must be recognised, however, that under some circumstances, photosynthesis would be Rubisco limited and could exhibit a stronger CO_2 response than calculated here.

The RuBP-regeneration-limited assimilation rate was calculated as:

$$w_j = \frac{J_{lim}(c_i - \Gamma_*)}{4(c_i + 2\Gamma_*)}, \tag{A9}$$

where c_i is the intercellular [CO_2], Γ_* the CO_2 compensation point in the absence of non-photorespiratory respiration and J_{lim} the light-limited rate of electron transport, calculated from a non-rectangular hyperbola as:

$$J_{lim} = \frac{\alpha I + J_{max} - \sqrt{(\alpha I + J_{max})^2 - 4\alpha I\theta J_{max}}}{2\theta}, \tag{A10}$$

where α is the quantum yield of electron transport, I is the absorbed photon flux density, J_{max} is the maximum rate of electron transport and θ is a curvature term in the relationship.

Absorbed photon flux density was then calculated as:

$$I = I_0\, e^{-Lk} \tag{A11}$$

where I_0 is incident photon flux density, L is leaf area index and k a light extinction coefficient [96].

Total absorbed net radiation, Q_a, was assumed to be proportional to absorbed photon flux density so that

$$Q_a = q\, I \tag{A12}$$

where q is a conversion factor between photosynthetically active radiation and total solar radiation, approximated as 0.5 [97].

Leaf area index, L, was calculated as:

$$L = p_l A_n \tag{A13}$$

where p_l is a proportionality term between photosynthetic carbon gain and leaf area index and A_n is net assimilation rate as defined in Eq. A8. Equation A13 created a circular interdependence between A_n and L that required an iterative computation sequence to be used to find overall convergence.

These relationship were used here with:

$$\alpha = 0.385 \tag{A14a}$$

$$I_0 = 500 \quad \left[\mu mol \ quanta \ m^{-2} s^{-1} \right] \tag{A14b}$$

$$J_{max} = 175 \quad \left[\mu mol \ m^{-2} s^{-1} \right] \tag{A14c}$$

$$\theta = 0.7 \tag{A14d}$$

$$k = 0.5 \tag{A14e}$$

$$p_l = 0.2 \tag{A14f}$$

In these equations, the intercellular $[CO_2]$, c_i, was calculated from the atmospheric $[CO_2]$ based on Eq. 5 in the main text.

Plant-based water use efficiency, W, was calculated simply as the ratio of canopy carbon gain over canopy transpirational water loss as:

$$W = A_n / A_{Tr} \tag{A15}$$

Future transpiration rates for specific sites

We obtained current climate information and expected climatic changes under different RCPs for six sites with contrasting current and expected future conditions. Current climatic data for these sites were obtained from https://cliflo.niwa.co.nz for New Zealand data; http://www.bom.gov.au/climate/averages/tables/cw_056238.shtml for Armidale, NSW, Australia; https://www.wunderground.com for the two US sites; http://www.manaus.climatemps.com/temperatures.php for Manuas, Brazil; and https://www.yr.no/place/Sweden/Other/Tiveden/statistics.html for Sweden.

The climate change scenarios are given for different RCPs and are based on simulations of the NOAA Geophysical Fluid Dynamics Laboratory (GFDL-CM3) Global Climate Model (GCM) that were prepared for the Coupled Model Intercomparison Project Phase 5 (CMIP5) [98]. The location of these sites is shown in Fig. 9.

These sites represented a range of contrasting conditions from very warm and humid in the tropical rainforest site to a very short growing season with a long and extremely cold winter at the boreal taiga site.

Monthly data for the grid cells encompassing each site was downloaded from https://esgf-node.llnl.gov/ and the following fields were extracted for the analyses: daily minimum and maximum surface air temperature, downwelling shortwave radiation, atmospheric pressure and specific humidity. Calculations of E_{Tr} and related variables were made directly from the monthly model output.

To determine and visualise trends in our simulations over the simulated period (2006 to 2100), data were first deseasonalised using the Seasonal Decomposition by Loess (stl) function in the R Stats (Version 3.4.1) and then smoothed using a 10-year running mean. At sites where growing season lengths were limited by cool temperatures, we weighted the E_{Tr} calculated for the month by the fraction of days within that month for which the daily minimum temperature exceeded 0 °C [79]. Growing season length was calculated by resampling monthly time series of simulated minimum temperatures to a daily time step using a spline function and calculating the number of days for which the minimum temperature exceeded 0 °C.

Appendix B. Verifying the daily approach to determining future E_{Tr} trajectories

Our analysis of future transpiration responses to climate change (Calculating Transpiration Rates, Transpiration Rates Under Changing $[CO_2]$ and Temperature, Discussion Sections) is based on an instantaneous daytime E_{Tr} that is calculated from Eq. A1 using projected climate variables aggregated at a daily time scale. However, inputs to Eq. A1 have large diurnal variations, and it was though possible that they could possibly interact in a highly non-linear manner. On sub-daily time scales, such interactions would not be captured by our calculation of E_{Tr} from daily data. If that had been the case, our approach using daily data as drivers might not have provided the best guide for E_{Tr} responses to future warming and $[CO_2]$ changes.

We investigated this issue by building two further sets of E_{Tr} that were based on a 12-month data set of
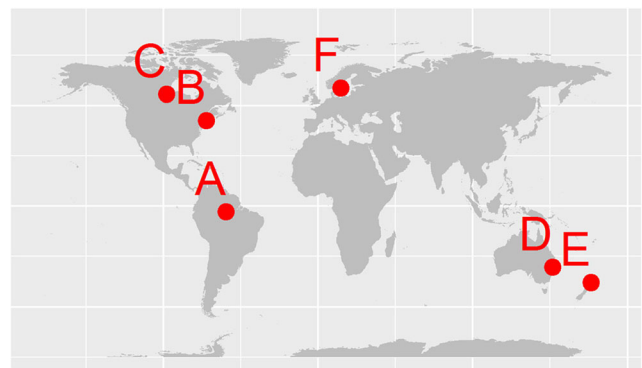

Fig. 9 Location of the six sites used to illustrate likely changes in transpiration rates for sites with different base climates. *A*: Tropical rainforest, Brazil; *B*: Temperate broadleaf, eastern USA; *C*: Boreal taiga, Canada; *D*: Temperate forest, Australia; *E*: Temperate forest, New Zealand; *F*: Temperate conifer, Europe

hourly observations from a co-located weather station and eddy covariance tower. We calculated:

1. Daily sums of E_{Tr} calculated at hourly time steps from measured input data (temperature, [CO_2], humidity, radiation and pressure)
2. Instantaneous E_{Tr} calculated from daily statistics derived from the hourly observations above but similar in form to those extracted from the CMIP5 output

We obtained 2013 weather data from a weather station maintained by New Zealand's National Institute of Water and Atmosphere and a co-located eddy covariance tower. The station and the tower were located over a dairy pasture site near Methven, Canterbury, New Zealand (43° 40′ S, 171° 35′ E) [99]. We used hourly mean temperatures, atmospheric pressure, wind speed and radiation, together with measured [CO_2]. The eddy covariance data provided direct [CO_2] measurements and other variables that are required to calculate r_a. We were then in a position to determine whether the non-linear interactions of driving variables on sub-daily time scales were sufficiently important to cast doubt on our conclusions (that were based on daily aggregations).

E_{Tr} calculated at daily time scales was calculated identically to the scheme described in Section "Calculating Transpiration Rates" and Appendix A. E_{Tr} calculated at hourly time scales used a similar scheme but hourly measurements of [CO_2], air temperature, specific humidity, pressure, radiation and aerodynamic resistance were used in Eq. A1a instead of daily estimates.

Aerodynamic resistance was calculated according to [100]:

$$r_a = \frac{1}{k_v^2 u}\left[\ln\left(\frac{Z-d}{Z_{0m}}\right)-\Psi_m(\varsigma,\varsigma_{0m})\right]\left[\ln\left(\frac{Z-d}{Z_{0h}}\right)-\Psi_h(\varsigma,\varsigma_{0h})\right]$$

$$(B1)$$

where k_v is the von Karman constant (0.41); u is the wind speed (m s^{-1}) at the reference height, Z (m); d is the zero plane displacement height (m); z_{0m} and z_{0h} are the aerodynamic roughness lengths for momentum and heat, respectively; $\Psi_m(\varsigma,\varsigma_{0m})$, $\Psi_H(\varsigma,\varsigma_{0h})$ are the stability correction functions (for momentum and heat, respectively) integrated between the reference height and the appropriate roughness length ($z_{0m \text{ or } z0h}$), and ς, ς_{0m}, ς_{0h} are dimensionless stability parameters, defined as $\varsigma = z/L$, $\varsigma_{0m} = z_{0m}/L$, and $\varsigma_{0h} = z_{0h}/L$, respectively, where $z = Z - d$ and L is the Obhukov length, calculated as:

$$L = \frac{-\rho_a C_p u_*^3 T_K}{k_v g H},$$

$$(B2)$$

where the friction velocity, u_*, the sensible heat, H, and T_K, the instantaneous air temperature in K ($T_K = T_{day} + 273.15$), were

obtained from the eddy covariance tower and ρ_a and C_p are the same terms used in Eq. A1, and g is the gravitational constant, 9.81 m s^{-2}.

To estimate wind speed at a reference height appropriate for forests, we used:

$$u = \frac{u_*}{k_v}\left[\ln\left(\frac{Z-d}{Z_{0m}}\right)-\Psi_m(\varsigma,\varsigma_{0m})\right].$$

$$(B3)$$

We used formulae for the integration of the stability functions under stable, neutral and unstable conditions from [101]. For the hourly estimates of the canopy resistance, r_c, we used the same sequence of equations [95–101] that was used for instantaneous calculations.

Calculated E_{Tr} values from both daily and hourly data were then averaged over the entire year. We repeated the analysis for a range of projected temperature and [CO_2] increases by adding fixed increments of temperature and [CO_2] to the corresponding data sets collected in 2013. The relative response for both instantaneous and daily data under these altered climate conditions is shown in Fig. 10.

The comparison between the two sets of simulations shows only small differences in the response to temperature changes and gave largely the same trends to changes in [CO_2], but the detailed full-day calculations resulted in marginally more conservative changes. For instance, at 900 ppm and with no temperature change, simulations based on point-simulations suggested reduced transpiration rates by about 40%, whereas the more detailed simulations gave reductions by only about 36% (Fig. 10). Similar differences were seen for the response to increasing [CO_2] at all different temperatures.

So, with trivial differences in the response to changing temperatures, and a difference of only 10% in the response
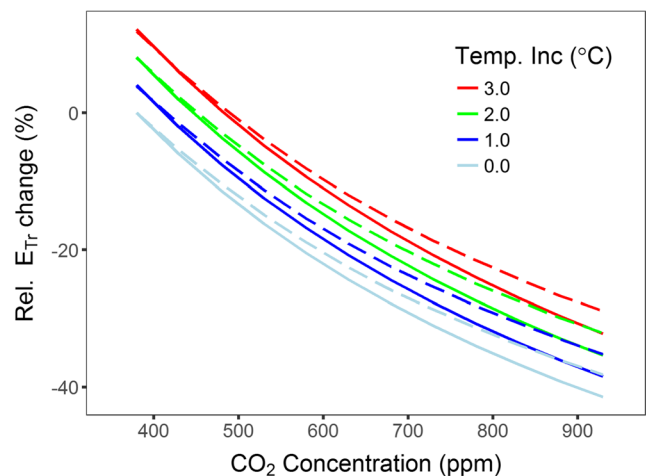

Fig. 10 Relative change in transpiration rates calculated for different combinations of changes in temperature and [CO_2]. Solid lines show simulations for transpiration rate estimates for one daily temperature value, summed over a year, and dashed lines show simulations with data based on hourly inputs. The initial CO_2 concentration is based on measured mean atmospheric [CO_2] value of 380 ppm

to changing [CO_2], we concluded that the role of non-linear interactions of E_{Tr} drivers on sub-daily time scales was relatively minor. This test thus validated the method of using instantaneous transpiration rates calculated from daily climate statistics to determine responses of E_{Tr} to changing temperature and [CO_2]. This was seen as the appropriate approach in order to retain clarity and transparency of the calculations.

Open Access This article is distributed under the terms of the Creative Commons Attribution 4.0 International License (http://creativecommons.org/licenses/by/4.0/), which permits unrestricted use, distribution, and reproduction in any medium, provided you give appropriate credit to the original author(s) and the source, provide a link to the Creative Commons license, and indicate if changes were made.

References

Papers of particular interest, published recently, have been highlighted as:
• Of importance
•• Of major importance

1. Collins M, Knutti R, Arblaster J, Dufresne J-L, Fichefet T, Friedlingstein P, et al. Long-term climate change: projections, commitments and irreversibility. In: Stocker TF, Qin D, Plattner G-K, Tignor M, Allen SK, Boschung J, Nauels A, Xia Y, Bex V, Midgley PM, editors. Climate change 2013: the physical science basis. Contribution of Working Group I to the Fifth Assessment Report of the Intergovernmental Panel on Climate Change. Cambridge: Cambridge University Press; 2013. p. 1029–136.
2. Kirschbaum MUF. Does enhanced photosynthesis enhance growth? Lessons learnt from CO_2 enrichments studies. Plant Physiol. 2011;155:117–24.
3. Franks PJ, Adams MA, Amthor JS, Barbour MM, Berry JA, Ellsworth DS, et al. Sensitivity of plants to changing atmospheric CO_2 concentration: from the geological past to the next century. New Phytol. 2013;197:1077–94.
4. Hickler T, Rammig A, Werner C. Modelling CO_2 impacts on forest productivity. Curr Forestry Rep. 2015;1:69–80.
5. Drake BG, Gonzalez-Meler MA, Long SP. More efficient plants: a consequence of rising atmospheric CO_2? Annu Rev Plant Phys. 1997;48:609–39.
6.•• MUF K, Lambie SM. Re-analysis of plant CO_2 responses during the exponential growth phase: interactions with light, temperature, nutrients and water availability. Funct Plant Biol. 2015;42:989–1000. **The authors reanalysed CO_2 growth experiments to remove the positive feedback during the exponential growth phase of plants and obtain unconfounded new estimates of the CO_2 response of plant growth. Previously, growth estimates had been inflated by positive feedback during exponential growth. The new estimates should correspond better to the true growth stimulation by CO_2.**
7. Ainsworth EA, Long SP. What have we learned from 15 years of free-air CO_2 enrichment (FACE)? A meta-analytic review of the responses of photosynthesis, canopy properties and plant production to rising CO_2. New Phytol. 2005;165:351–71.
8. Norby RJ, DeLucia EH, Gielen B, Calfapietra C, Giardina CP, King JS, et al. Forest response to elevated CO_2 is conserved across a broad range of productivity. PNAS. 2005;102:18052–6.
9. Gedney N, Cox PM, Betts RA, Boucher O, Huntingford C, Stott PA. Detection of a direct carbon dioxide effect in continental river runoff records. Nature. 2006;439:835–8.
10. McMurtrie RE, Norby RJ, Medlyn BE, Dewar RC, Pepper DA, Reich PB, et al. Why is plant-growth response to elevated CO_2 amplified when water is limiting, but reduced when nitrogen is limiting? A growth-optimisation hypothesis. Funct Plant Biol. 2008;35:521–34.
11. van Vuuren DP, Edmonds J, Kainuma M, Riahi K, Thomson A, Hibbard K, et al. The representative concentration pathways: an overview. Clim Chang. 2011;109:5–31.
12. Trenberth KE, Jones PD, Ambenje P, Bojariu R, Easterling D, Klein Tank A, et al. Surface and atmospheric climate change. In: Solomon S, Qin D, Manning M, Chen Z, Marquis M, Averyt KB, Tignor M, Miller HL, editors. Climate change 2007: the physical science basis. Contribution of Working Group I to the Fourth Assessment Report of the Intergovernmental Panel on Climate Change. Cambridge: Cambridge University Press; 2007. p. 235–336.
13. Kirschbaum MUF. Forest growth and species distributions in a changing climate. Tree Physiol. 2000;20:309–22.
14. Martin P, Rosenberg N, McKenney MS. Sensitivity of evapotranspiration in a wheat field, a forest and a grassland to changes in climate and direct effects of carbon dioxide. Clim Chang. 1989;14:117–51.
15. McKenney MS, Rosenberg NJ. Sensitivity of some potential evapotranspiration estimation methods to climate change. Agric For Meteorol. 1993;64:81–110.
16.• Swann ALS, Hoffman FM, Koven CD, Randerson JT. Plant responses to increasing CO_2 reduce estimates of climate impacts on drought severity. PNAS. 2016;113:10019–24. **The authors modelled future drought incidence by explicitly including stomatal conductance in their calculation. That reduced inferred drought incidence and demonstrated the crucial role of that plant physiological factor.**
17.• Milly PCD, Dunne KA. Potential evapotranspiration and continental drying. Nat Clim Change. 2016;6:946–9. **The authors modelled changes in evapotranspiration rates by explicitly including stomatal conductance in their calculation. That reduced inferred increases in future transpiration rates. It added to the work of Swann et al. (2016) by clearly demonstrating the crucial role of changes in stomatal conductance.**
18. Hasper TB, Wallin G, Lamba S, Hall M, Jaramillo F, Laudon H, et al. Water use by Swedish boreal forests in a changing climate. Funct Ecol. 2016;30:690–9.
19. Dai A, Trenberth KE, Qian T. A global data set of Palmer Drought Severity Index for 1870–2002: relationship with soil moisture and effects of surface warming. J Hydrometeorol. 2004;5:1117–30.
20. Briffa KR, van der Schrier G, Jones PD. Wet and dry summers in Europe since 1750: evidence of increasing drought. Int J Climatol. 2009;29(13):1894–905.
21. Lutz JA, van Wagtendonk JW, Franklin JF. Climatic water deficit, tree species ranges, and climate change in Yosemite National Park. J Biogeogr. 2010;37:936–50.
22. Seager R, Ting MF, Li CH, Naik N, Cook B, Nakamura J, et al. Projections of declining surface-water availability for the southwestern United States. Nat Clim Chang. 2013;3:482–6.
23. Sheffield J, Wood EF, Roderick ML. Little change in global drought over the past 60 years. Nature. 2012;491:435–8.
24. Trenberth KE, Dai AG, van der Schrier G, Jones PD, Barichivich J, Briffa KR, et al. Global warming and changes in drought. Nat Clim Chang. 2014;4:17–22.
25.• Zhang J, Sun FB, Xu JJ, Chen YN, Sang YF, Liu CM. Dependence of trends in and sensitivity of drought over China (1961–2013) on potential evaporation model. Geophys Res Lett. 2016;43:206–13. **The authors used different models to model**

changes in drought over China and showed that a mechanistic formulation (Penman-Monteith) resulted in reductions in calculated changes whereas purely empirically-based formulations (Thornthwaite) resulted in increases in transpiration rates. This was an important contribution by explicitly demonstrating important differences in drought predictions based purely on the choice of calculation method.

26. Cook B, Smerdon J, Seager R, Coats S. Global warming and 21st century drying. Clim Dyn. 2014;43:2607–27.

27. Farquhar GD, von Caemmerer S, Berry J. A biochemical model of photosynthetic CO_2 assimilation in leaves of C_3 species. Planta. 1980;149:78–90.

28. McMahon TA, Peel MC, Lowe L, Srikanthan R, McVicar TR. Estimating actual, potential, reference crop and pan evaporation using standard meteorological data: a pragmatic synthesis. Hydrol Earth Syst Sci. 2013;17:1331–63.

29. Thornthwaite CW. An approach towards a rational classification of climate. Geograph Rev. 1948;38:55–94.

30. Monteith JL. Evaporation and environment. Sym Soc Exp Biol. 1965;19:205–34.

31. Allen RG, Pereira LS, Raes D, Smith M. Crop evapotranspiration: guidelines for computing crop water requirements. FAO Irrigation and Drainage Paper no. 56, Rome, Italy. 1998.

32. Morison JIL. Sensitivity of stomata and water use efficiency to high CO_2. Plant Cell Environ. 1985;8:467–74.

33. Allen LH. Plant responses to rising carbon dioxide and potential interactions with air pollutants. J Environ Qual. 1990;19:15–34.

34. Eamus D. The interaction of rising CO_2 and temperatures with water-use efficiency. Plant Cell Environ. 1991;14:843–52.

35. Field CB, Jackson RB, Mooney HA. Stomatal responses to increased CO_2: implications from the plant to the global-scale. Plant Cell Environ. 1995;18:1214–25.

36. Urban O. Physiological impacts of elevated CO_2 concentration ranging from molecular to whole plant responses. Photosynthetica. 2003;41:9–20.

37. Medlyn BE, Barton CVM, Broadmeadow MSJ, Ceulemans R, De Angelis P, Forstreuter M, et al. Stomatal conductance of forest species after long-term exposure to elevated CO_2 concentration: a synthesis. New Phytol. 2001;149:247–64.

38. Curtis PS, Wang X. A meta analysis of elevated CO_2 effects on woody plant mass, form, and physiology. Oecologia. 1998;113:299–313.

39. Ball JT, Woodrow IE, Berry JA. A model predicting stomatal conductance and its contribution to the control of photosynthesis under different environmental conditions. In: Biggins J, editor. Progress in photosynthesis research. Dordrecht: Martin-Nijhoff Publishers; 1987. p. 221–4.

40. Woodward FI, Kelly CK. The influence of CO_2 concentration on stomatal density. New Phytol. 1995;131:311–27.

41. Woodward FI. Stomatal numbers are sensitive to increases in CO_2 from pre-industrial levels. Nature. 1987;327:617–8.

42. Lammertsma EI, de Boer HJ, Dekker SC, Dilcher DL, Lotter AF, Wagner-Cremer F. Global CO_2 rise leads to reduced maximum stomatal conductance in Florida vegetation. PNAS. 2011;108:4035–40.

43. Steinthorsdottir M, Wohlfarth B, Kylander ME, Blaauw M, Reimer PJ. Stomatal proxy record of CO_2 concentrations from the last termination suggests an important role for CO_2 at climate change transitions. Quat Sci Rev. 2013;68:43–58.

44. Cernusak LA, Ubierna N, Winter K, Holtum JAM, Marshall JD, Farquhar GD. Environmental and physiological determinants of carbon isotope discrimination in terrestrial plants. New Phytol. 2013;200:950–65.

45. Dawson TE, Mambelli S, Plamboeck AH, Templer PH, Tu KP. Stable isotopes in plant ecology. Annu Rev Ecol Syst. 2002;33:507–59.

46. Duquesnay A, Breda N, Stievenard M, Dupouey JL. Changes of tree-ring $\delta^{13}C$ and water-use efficiency of beech (*Fagus sylvatica* L.) in north-eastern France during the past century. Plant Cell Environ. 1998;21:565–72.

47. Arneth A, Lloyd J, Santruckova H, Bird M, Grigoryev S, Kalaschnikov YN, et al. Response of central Siberian Scots pine to soil water deficit and long-term trends in atmospheric CO_2 concentration. Glob Biogeochem Cycles. 2002;16:1–13.

48. Saurer M, Siegwolf RTW, Schweingruber FH. Carbon isotope discrimination indicates improving water-use efficiency of trees in northern Eurasia over the last 100 years. Glob Chang Biol. 2004;10:2109–20.

49. Frank DC, Poulter B, Saurer M, Esper J, Huntingford C, Helle G, et al. Water-use efficiency and transpiration across European forests during the Anthropocene. Nat Clim Chang. 2015;5:579–83.

50. Marshall JD, Monserud RA. Homeostatic gas-exchange parameters inferred from $^{13}C/^{12}C$ in tree rings of conifers. Oecologia. 1996;105:13–21.

51. Monserud RA, Marshall JD. Time-series analysis of $\delta^{13}C$ from tree rings. I. Time trends and autocorrelation. Tree Physiol. 2001;21:1087–102.

52.•• Keenan TF, Hollinger DY, Bohrer G, Dragoni D, Munger JW, Schmid HP, et al. Increase in forest water-use efficiency as atmospheric carbon dioxide concentrations rise. Nature. 2013;499:324–7. **The authors compiled data from long-term eddy covariance systems and demonstrated increasing water-use efficiency in line with naturally-changing background CO_2 concentrations. This was an important contribution by using explicit observations of plant canopies under natural conditions to demonstrate the effect of CO_2 concentration on water-use efficiency.**

53. Dekker SC, Groenendijk M, Booth BBB, Huntingford C, Cox PM. Spatial and temporal variations in plant water-use efficiency inferred from tree-ring, eddy covariance and atmospheric observations. Earth Syst Dyn. 2016;7:525–33.

54. Wils THG, Robertson I, Woodborne S, Hall G, Koprowski M, Eshetu Z. Anthropogenic forcing increases the water-use efficiency of African trees. J Quart Sci. 2016;31:386–90.

55. Labat D, Gedderis Y, Probst JL, Guyot JL. Evidence for global runoff increase related to climate warming. Adv Water Resour. 2004;27:631–42.

56. Piao SL, Friedlingstein P, Ciais P, de Noblet-Ducoudre N, Labat D, Zaehle S. Changes in climate and land use have a larger direct impact than rising CO_2 on global river runoff trends. PNAS. 2007;104:15242–7.

57. Donohue RJ, TR MV, Roderick ML. Climate-related trends in Australian vegetation cover as inferred from satellite observations, 1981-2006. Glob Chang Biol. 2009;15:1025–39.

58. Dardel C, Kergoat L, Hiernaux P, Grippa M, Mougin E, Ciais P, et al. Rain-use-efficiency: what it tells us about the conflicting Sahel greening and Sahelian paradox. Remote Sens. 2014;6:3446–74.

59. Schut AGT, Ivits E, Conijn JG, ten Brink B, Fensholt R. Trends in global vegetation activity and climatic drivers indicate a decoupled response to climate change. PLOS One. 2015;10:e0138013.

60.•• Donohue RJ, Roderick ML, McVicar TR, Farquhar GD. Impact of CO_2 fertilization on maximum foliage cover across the globe's warm, arid environments. Geophys Res Lett. 2013;40:3031–5. **The authors used remotely sensed data to record changes in leaf area in warm and arid regions of the world and relate the documented changes to increasing CO_2 concentration. The study was restricted to conditions where other factors, like temperature, were considered to be either unlimiting or explicitly accounted for, like precipitation. It was an important contribution by explicitly demonstrating the enhancement of**

water-use efficiency by elevated CO₂ with a data set covering a wide geographical area.

61. Samarakoon AB, Gifford RM. Soil water content under plants at high CO₂ concentration and interactions with the direct CO₂ effects: a species comparison. J Biogeogr. 1995;22:193–202.

62. Robredo A, Perez-Lopez U, de la Maza HS, Gonzalez-Moro B, Lacuesta M, Mena-Petite A, et al. Elevated CO₂ alleviates the impact of drought on barley improving water status by lowering stomatal conductance and delaying its effects on photosynthesis. Environ Exp Bot. 2007;59:252–63.

63. Wullschleger SD, Tschaplinski TJ, Norby RJ. Plant water relations at elevated CO₂—implications for water-limited environments. Plant Cell Environ. 2002;25:319–31.

64. Ainsworth EA, Rogers A. The response of photosynthesis and stomatal conductance to rising [CO₂]: mechanisms and environmental interactions. Plant Cell Environ. 2007;30:258–70.

65. Morgan JA, Pataki DE, Körner C, Clark H, Del Grosso SJ, Grünzweig JM, et al. Water relations in grassland and desert ecosystems exposed to elevated atmospheric CO₂. Oecologia. 2004;140:11–2.

66. van der Kooi CJ, Reich M, Low M, De Kok LJ, Tausz M. Growth and yield stimulation under elevated CO₂ and drought: a meta-analysis on crops. Environ Exp Bot. 2016;122:150–7.

67. Leakey ADB, Ainsworth EA, Bernacchi CJ, Rogers A, Long SP, Ort DR. Elevated CO₂ effects on plant carbon, nitrogen, and water relations: six important lessons from FACE. J Exp Bot. 2009;60:2859–76.

68. Nowak RS, Ellsworth DS, Smith SD. Functional responses of plants to elevated atmospheric CO₂—do photosynthetic and productivity data from FACE experiments support early predictions? New Phytol. 2004;162:253–80.

69. Carthy HR, Oren R, Johnsen KH, Gallet-Budynek A, Pritchard SG, Cook CW, et al. Re-assessment of plant carbon dynamics at the Duke free-air CO₂ enrichment site: interactions of atmospheric [CO₂] with nitrogen and water availability over stand development. New Phytol. 2010;185:514–28.

70. Gunderson CA, Wullschleger SD. Photosynthetic acclimation in trees to rising atmospheric CO₂: a broader perspective. Photosynth Res. 1994;39:369–88.

71. McGuire AD, Melillo JM, Joyce LA. The role of nitrogen in the response of forest net primary production to elevated atmospheric carbon dioxide. Annu Rev Ecol Syst. 1995;26:473–503.

72. Medlyn BE, Badeck FW, De Pury DGG, Barton CVM, Broadmeadow M, Ceulemans R, et al. Effects of elevated [CO₂] on photosynthesis in European forest species: a meta-analysis of model parameters. Plant Cell Environ. 1999;22:1475–95.

73. Arora VK, Boer GJ, Christian JR, Curry CL, Denman KL, Zahariev K, et al. The effect of terrestrial photosynthesis down regulation on the twentieth-century carbon budget simulated with the CCCma Earth System Model. J Clim. 2009;22:6066–88.

74. Arp WJ. Effects of source sink relations on photosynthetic acclimation to elevated carbon dioxide. Plant Cell Environ. 1991;14:869–76.

75. Luo Y, Su B, Currie WS, Dukes JS, Finzi A, Hartwig U, et al. Progressive nitrogen limitation of ecosystem responses to rising atmospheric carbon dioxide. Biosci. 2004;54:731–9.

76. Gill RA, Anderson LJ, Polley HW, Johnson HB, Jackson RB. Potential nitrogen constraints on soil carbon sequestration under low and elevated atmospheric CO₂. Ecology. 2006;87:41–52.

77. Comins HN, McMurtrie RE. Long-term response of nutrient-limited forests to CO₂ enrichment—equilibrium behavior of plant-soil models. Ecol Appl. 1993;3:666–81.

78. Kirschbaum MUF. Direct and indirect climate-change effects on photosynthesis and transpiration. Plant Biol. 2004;6:242–53.

79. Kerkhoff AJ, Enquist BJ, Elser JJ, Fagan WF. Plant allometry, stoichiometry and productivity. Glob Ecol Biogeogr. 2005;14:585–98.

80. Baldocchi D, Ma SY. How will land use affect air temperature in the surface boundary layer? Lessons learned from a comparative study on the energy balance of an oak savanna and annual grassland in California, USA. Tellus Ser B. 2013;65:19994.

81. Jarvis PG, McNaughton KG. Stomatal control of transpiration—scaling up from leaf to region. Adv Ecol Res. 1986;15:1–49.

82. Kirschbaum MUF. Modelling forest growth and carbon storage with increasing CO₂ and temperature. Tellus Ser B. 1999;51B:871–88.

83. Körner C, Morgan J, Norby R. CO₂ fertilization: when, where, how much? In: Canadell JG, Pataki DE, Pitelka LF, editors. Terrestrial ecosystems in a changing world. Berlin: Springer Verlag; 2007. p. 9–21.

84. Shuttleworth WJ, Wallace JS. Evaporation from sparse crops—an energy combination theory. Q J R Meteorol Soc. 1985;111:839–55.

85. Kirschbaum MUF, Rutledge S, Kuijper IA, Mudge PL, Puche N, Wall AM, et al. Modelling carbon and water exchange of a grazed pasture in New Zealand constrained by eddy covariance measurements. Sci Tot Environ. 2015;512:273–86.

86. Roderick ML, Greve P, Farquhar GD. On the assessment of aridity with changes in atmospheric CO₂. Water Resour Res. 2015;51:5450–63.

87. Milly PCD, Betancourt J, Falkenmark M, Hirsch RM, Kundzewicz ZW, Lettenmaier DP, et al. Stationarity is dead: whither water management? Science. 319:573–4.

88. Dai AG. Increasing drought under global warming in observations and models. Nat Clim Chang. 2003;3:52–8.

89. Williams AP, Allen CD, Macalady AK, Griffin D, Woodhouse CA, Meko DM, et al. Temperature as a potent driver of regional forest drought stress and tree mortality. Nat Clim Chang. 2013;3:292–7.

90. Dai AG. Drought under global warming: a review. Wiley Interdiscip Rev Clim Chang. 2010;2:45–65.

91. Cox PM, Betts RA, Bunton CB, Essery RLH, Rowntree PR, Smith J. The impact of new land surface physics on the GCM simulation of climate and climate sensitivity. Clim Dyn. 1999;15:183–203.

92. Boucher O, Jones A, Betts RA. Climate response to the physiological impact of carbon dioxide on plants in the Met Office Unified Model HadCM3. Clim Dyn. 2009;32:237–49.

93. Cao L, Bala G, Cadeira K, Nemani R, Ban-Weiss G. Importance of carbon dioxide physiological forcing to future climate change. PNAS. 2010;107:9513–8.

94. Bonan G. Ecological climatology—concepts and applications. 2nd ed. Cambridge: University Press; 2002.

95. Kirschbaum MUF, Farquhar GD. Temperature dependence of whole-leaf photosynthesis in Eucalyptus pauciflora Sieb. ex Spreng. Aust J Plant Physiol. 1984;11:519–38.

96. Zhang LX, Hu ZM, Fan JW, Zhou DC, Tang FP. A meta-analysis of the canopy light extinction coefficient in terrestrial ecosystems. Front Earth Sci. 2014;8:599–609.

97. Ross J, Sulev M. Sources of errors in measurements of PAR. Agric For Meteorol. 2000;100:103–25.

98. Taylor KE, Stouffer RJ, Meehl GA. An overview of CMIP5 and the experiment design. Bull Amer Meteor Soc. 2012;93:485–98.

99. Graham SL, Kochendorfer J, McMillan AMS, Duncan MJ, Srinivasan MS, Hertzog G. Effects of agricultural management on measurements, prediction, and partitioning of evapotranspiration in irrigated grasslands. Agric Water Manag. 2016;177:340–7.

100. Thom AS. Momentum, mass and heat exchange of plant communities. In: Monteith JL, editor. Vegetation and the atmosphere. London: Academic Press; 1975. p. 57–109.

101. Liu S, Lu L, Mao D, Jia L. Evaluating parameterizations of aerodynamic resistance to heat transfer using field measurements. Hydrol Earth Syst Sci. 2007;11:769–83.